Critical Literature Review of High-Performance Corrosion Reinforcements in Concrete Bridge Applications

Final Report
July 2004

FHWA-HRT-04-093

FOREWORD

Economic considerations historically have precluded consideration and widespread utilization of high-performance (corrosion-resistant) reinforcements (such as stainless steels) in bridge construction. However, with the advent of life cycle cost analysis as a project planning tool and of a requirement that major bridge structures have a 75−100-year design life, the competitiveness of such steels has increased such that enhanced attention has been focused upon these materials in recent years.

This investigation was initiated to evaluate the corrosion resistance of various categories of high-performance reinforcement, including new products that are becoming available, in bridge structures that are exposed to chlorides. Both long-term (4-year) test yard exposures and accelerated laboratory experiments in simulated concrete pore waters were involved. The ultimate objective is to: (1) evaluate the corrosion properties and rank the different candidate materials; and (2) develop tools and short-term tests to help practitioners project long-term performance in actual structures. This interim report presents the results of a critical literature review of corrosion issues and behavior for high-performance reinforcements as applicable to bridges and as a precursor to the experimental program.

T. Paul Teng, P.E.
Director, Office of Infrastructure
Research and Development

NOTICE

1. Report No. FHWA-HRT-04-093	2. Government Accession No.	3. Recipient's Catalog No.
4. Title and Subtitle A Critical Literature Review of High-Performance Corrosion Reinforcements in Concrete Bridge Applications		5. Report Date July 2004
		6. Performing Organization Code FAU-OE-CMM-04
7. Author(s) William H. Hartt,* Rodney G. Powers,** Virginie Leroux,* and Diane K. Lysogorski* (See box 15)		8.Performing Organization Report No.
9. Performing Organization Name and Address Center for Marine Materials Florida Atlantic University—Sea Tech Campus 101 North Beach Road Dania Beach, FL 33004		10. Work Unit No. (TRAIS)
		11. Contract or Grant No.
12. Sponsoring Agency Name and Address Office of Infrastructure Research and Development Federal Highway Administration 6300 Georgetown Pike McLean, VA 22012-2296		13. Type of Report and Period Covered Interim Report
		14. Sponsoring Agency Code

15. Supplementary Notes
Contracting Officer's Technical Representative (COTR): Y.P. Virmani, HRDI-10 * Center for Marine Materials Florida Atlantic University—Sea Tech Campus 101 North Beach Road, Dania Beach, FL 33004 ** Florida Department of Transportation State Materials Office 5007 NE 39th Street Gainesville, FL 32609

16. Abstract
A critical literature review regarding high-performance reinforcement for concrete bridge applications was conducted. This included (1) an overview of the corrosion-induced concrete deterioration process, (2) corrosion control alternatives, (3) the utility of corrosion (pitting) resistant alloys for applications in chloride containing environments, (4) a review of the pitting mechanism, and (5) performance of various metallic reinforcement types in aqueous solutions, cementitious embedments, test yard exposures, and actual structures. Specific alloys upon which attention was directed include black steel; MMFX-II; and various grades of ferritic, austenitic, and duplex stainless steels, as both solid and clad bars and in the as-received and pickled conditions. It was determined that the high-performance alloys outperformed black steel from a corrosion resistance standpoint. Unlike the various grades of black steel, however, a relatively wide range of corrosion performance was apparent for the high-performance counterparts depending upon the alloy and surface condition. At the same time, the present approach to materials selection for bridge construction is to identify the reinforcement candidate that will achieve the design life at the least life cycle cost. This, in turn requires that long-term corrosion performance of candidate reinforcement types be known for the anticipated design life of the bridge in question, which can be 75–100 years. However, because service history for these materials in this application is limited, the necessary information can only be obtained from accelerated, short-term tests, but there is no reliable correlation between the results from these tests and long-term performance.

Key Words Reinforced concrete, bridges, corrosion resistance, high-performance reinforcement, stainless steels, MMFX-II		18. Distribution Statement No restrictions. This document is available to the public through NTIS, Springfield, VA 22161	
19. Security Classif. (of this report) Unclassified	20. Security Classif. (of this page) Unclassified	21.No of Pages 54	22. Price

Form DOT F 1700.7   (8-72)   Reproduction of completed page authorized

SI* (MODERN METRIC) CONVERSION FACTORS

APPROXIMATE CONVERSIONS TO SI UNITS

Symbol	When You Know	Multiply By	To Find	Symbol
LENGTH				
in	inches	25.4	millimeters	mm
ft	feet	0.305	meters	m
yd	yards	0.914	meters	m
mi	miles	1.61	kilometers	km
AREA				
in^2	square inches	645.2	square millimeters	mm^2
ft^2	square feet	0.093	square meters	m^2
yd^2	square yard	0.836	square meters	m^2
ac	acres	0.405	hectares	ha
mi^2	square miles	2.59	square kilometers	km^2
VOLUME				
fl oz	fluid ounces	29.57	milliliters	mL
gal	gallons	3.785	liters	L
ft^3	cubic feet	0.028	cubic meters	m^3
yd^3	cubic yards	0.765	cubic meters	m^3
NOTE: volumes greater than 1000 L shall be shown in m^3				
MASS				
oz	ounces	28.35	grams	g
lb	pounds	0.454	kilograms	kg
T	short tons (2000 lb)	0.907	megagrams (or "metric ton")	Mg (or "t")
TEMPERATURE (exact degrees)				
^oF	Fahrenheit	5 (F-32)/9 or (F-32)/1.8	Celsius	^oC
ILLUMINATION				
fc	foot-candles	10.76	lux	lx
fl	foot-Lamberts	3.426	candela/m^2	cd/m^2
FORCE and PRESSURE or STRESS				
lbf	poundforce	4.45	newtons	N
lbf/in^2	poundforce per square inch	6.89	kilopascals	kPa

APPROXIMATE CONVERSIONS FROM SI UNITS

Symbol	When You Know	Multiply By	To Find	Symbol
LENGTH				
mm	millimeters	0.039	inches	in
m	meters	3.28	feet	ft
m	meters	1.09	yards	yd
km	kilometers	0.621	miles	mi
AREA				
mm^2	square millimeters	0.0016	square inches	in^2
m^2	square meters	10.764	square feet	ft^2
m^2	square meters	1.195	square yards	yd^2
ha	hectares	2.47	acres	ac
km^2	square kilometers	0.386	square miles	mi^2
VOLUME				
mL	milliliters	0.034	fluid ounces	fl oz
L	liters	0.264	gallons	gal
m^3	cubic meters	35.314	cubic feet	ft^3
m^3	cubic meters	1.307	cubic yards	yd^3
MASS				
g	grams	0.035	ounces	oz
kg	kilograms	2.202	pounds	lb
Mg (or "t")	megagrams (or "metric ton")	1.103	short tons (2000 lb)	T
TEMPERATURE (exact degrees)				
^oC	Celsius	1.8C+32	Fahrenheit	^oF
ILLUMINATION				
lx	lux	0.0929	foot-candles	fc
cd/m^2	candela/m^2	0.2919	foot-Lamberts	fl
FORCE and PRESSURE or STRESS				
N	newtons	0.225	poundforce	lbf
kPa	kilopascals	0.145	poundforce per square inch	lbf/in^2

*SI is the symbol for the International System of Units. Appropriate rounding should be made to comply with Section 4 of ASTM E380.
(Revised March 2003)

TABLE OF CONTENTS

LIST OF FIGURES

LIST OF TABLES

INTRODUCTION

General

The United States has a major investment in its highway system; the system's performance, in conjunction with that of other transportation modes, is critical to the Nation's economic health and societal functioning. Although deterioration of structures over time is normal and expected, the rate at which this has occurred for highway bridges since the 1960s, when officials began applying deicing salts in northern locations in the winter, has been abnormally advanced and has posed significant challenges, both economically and technically. Also important is the fact that similar advanced deterioration has occurred for bridges in coastal locations, both northern and southern, because of seawater or spray exposure. In both cases (deicing salts and marine exposure), the deterioration is a consequence of the aggressive nature of the chloride ion.[1] More than half of the total bridge inventory in the United States is reinforced concrete, and these structures have proved to be particularly susceptible to deterioration. A recent study has indicated that the annual direct cost of corrosion to bridges is 5.9-9.7B\$.[2] If indirect factors are included also, this cost can be as mush as 10 times higher than that estimate.[3]

As this problem has manifested itself during the past 40 years, technical efforts have been directed toward first, understanding the deterioration mechanism and second, developing prevention and intervention strategies. The objective of the present review is to evaluate efforts in both categories from the perspective of high-performance (corrosion-resistant) reinforcing steel for concrete bridge deck and substructure service.

Overview of Corrosion-Induced Concrete Deterioration Processes

General

Although concrete has evolved to become the most widely used structural material in the world, the fact that its capacity for plastic deformation (so its ability to absorb mechanically imparted energy is essentially nil) imposes major practical service limitations. This shortcoming most commonly is overcome by incorporating steel reinforcement into specific locations in the concrete where tensile stresses are anticipated. Consequently, concerns regarding performance must not only focus upon properties of the concrete but also of the embedded steel and, in addition, the manner in which these two components interact. In this regard, steel and concrete are, in most aspects, mutually compatible, as exemplified by the fact that the coefficient of thermal expansion for each is approximately the same. Also, while boldly exposed steel corrodes actively in most natural environments at a rate that requires instituting extrinsic corrosion control measures (for example, protective coatings for atmospheric exposures and cathodic protection in submerged and buried situations), the relatively high pH of concrete pore water (pH $\approx$ 13.0–13.8) helps form a protective oxide (passive) film about 10 nanometers thick. This film effectively insulates the metal and electrolytes so that the corrosion rate is negligible, allowing decades of relatively low maintenance.

Corrosion Mechanism

Disrupting the passive film upon embedded reinforcement and onset of active corrosion can arise in conjunction with either of two causes: carbonation or chloride intrusion (or a combination of the two). In the case of carbonation, atmospheric carbon dioxide (CO_2) reacts with pore water alkali according to the generalized reaction,

$$Ca(OH)_2 + CO_2 \rightarrow CaCO_3 + H_2O, \tag{1}$$

which consumes reserve alkalinity and reduces pore water pH to the 8–9 range, where steel is no longer passive. For dense, high-quality concrete (for example, high cement factor, low water-cement ratio, and pozzolanic admixture), carbonation rates are typically on the order of 1 mm per decade or less; loss of passivity from this cause within a normal design life is not generally a concern. Carbonation must be anticipated at concrete cracks, however, where air essentially has direct access to the reinforcement, irrespective of concrete cover and quality. Older structures are also at issue because of their age, because earlier generation concretes were typically more permeable when compared to more recent concretes, and because of relatively low concrete cover.

Chlorides, on the other hand, arise in conjunction with deicing activities upon northern roadways or from coastal exposure, as noted above. While this species (Cl^-) has only a small influence on pore water pH, concentrations as low as 0.6 kilograms per cubic meter (kg/m^3) (concrete weight basis) have been projected to compromise steel passivity. In actuality, it probably is not the concentration of chlorides that governs loss of passivity but rather the ratio of chlorides-to-hydroxides ($[Cl^-]/[OH^-]$), because the latter species (OH^-) acts as an inhibitor. This has been demonstrated by aqueous solution experiments from which it is apparent that the Cl^- threshold for loss-of-steel passivity increased with increasing pH.[4–5] However, in cementitious materials, this interrelationship is more complex due to Cl^- binding and the dependence of such binding upon pH.[6] Thus, Cl^- binding evidently decreases with increasing OH^- above pH 12.6, such that a decrease in pH can result in decreasing $[Cl^-]/[OH^-]$.[7] Considerable research efforts have focused on identifying a chloride threshold; however, a unique value for this parameter has remained elusive, presumably because of the numerous influential variables, including type of cement, cement alkalinity, concrete mix design, environmental factors, potential, and reinforcement composition and microstructure.[8] Because Cl^-, not carbonation-induced loss of passivity, is of primary concern for bridge structures, subsequent focus is placed upon this cause of corrosion alone.

After steel in concrete becomes active, either in conjunction with chlorides achieving the threshold concentration or pore solution pH reduction from carbonation at the embedded steel depth, then the classical anodic iron reaction,

$$Fe \rightarrow Fe^{+2} + 2e^-, \tag{2}$$

and cathodic oxygen reduction reaction,

$$\frac{1}{2}O_2 + H_2O + 2e^- \rightarrow 2OH^-, \tag{3}$$

occur at an accelerated rate. Ferrous ions subsequently react to form sequential oxides according to

$$Fe^{+2} + 2OH^- \rightarrow Fe(OH)_2 \text{ and} \tag{4}$$

$$2Fe(OH)_2 + \frac{1}{2}O_2 \rightarrow 2\gamma - FeOOH + H_2O, \tag{5}$$
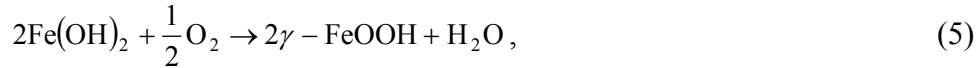
where the latter ferric product (γ–FeOOH) is more protective than the ferrous. Because the ferrous-to-ferric conversion occurs over time and is never complete, passive film disruptions invariably are present. In addition, neither product is protective in the presence of Cl⁻ or at pH below about 11.5.[9] Despite the normally high alkalinity of concrete, acidification may occur in the vicinity of anodic sites because of oxygen depletion and hydrolysis of ferrous ions.[1] Thus,

$$Fe^{+2} + 2H_2O \rightarrow Fe(OH)_2 + 2H^+ \tag{6}$$

The product H⁺ may be reduced and, along with O_2 reduction at more remote cathodic sites, further accelerate the anodic process. Further oxidation can occur as

$$4Fe(OH)_2 + 2H_2O + O_2 \rightarrow 4Fe(OH)_3 \text{ and} \tag{7}$$

$$2Fe(OH)_3 \rightarrow Fe_2O_3 + 3H_2O \tag{8}$$

Interestingly, corrosion seldom causes failure in reinforced concrete components and structures. Failure occurs because the oxide products (ferrous and ferric) have specific volumes that are multiples of that of the reactant steel; their accumulation in the concrete pore space adjacent to anodic sites leads to development of tensile hoop stresses around steel which, in combination with the relatively low tensile strength of concrete (typically 1–2 megapascals (MPa)), ultimately cause cracking and spalling. Figure 1 shows a photograph of corrosion-induced concrete spalling on a bridge piling in Florida.

Figure 1. Photograph of a cracked and spalled marine bridge piling.

Because corrosion-induced deterioration is progressive, inspections for damage assessment must be performed routinely; present Federal guidelines require a visual inspection every 2 years.[10] Because the corrosion is progressive and the resultant damage distributed in severity, repairs are needed continually. If such visual indicators are not addressed, then public safety is at risk. As an example, corrosion-induced concrete spalls occur as potholes in a bridge deck and contribute to unsafe driving conditions. As an extreme, structural failure and collapse may occur.

The situation is more critical and challenging in the case of post-tensioned structures, where advanced corrosion often is not revealed by visual inspection and loss of tendons is more critical to integrity than in the case of conventional reinforcement. Here, nondestructive testing methods such as magnetic flux leakage and natural frequency measurements are helpful, but these do not address all aspects of the problem and are expensive to apply.

Representation of Corrosion-Induced Concrete Deterioration

Corrosion-induced deterioration of reinforced concrete can be modeled in terms of three component steps: (1) time for corrosion initiation, T_i; (2) time, subsequent to corrosion initiation, for appearance of a crack on the external concrete surface (crack propagation), T_p; and (3) time for surface cracks to progress into further damage and develop into spalls, T_d, to the point where the functional service life, T_f, is reached.[11] Figure 2 illustrates these schematically as a plot of cumulative damage versus time. Of the life component terms, T_i occupies the longest period in most cases, so corrosion control measures generally focus on this parameter. In the case of epoxy-coated reinforcement, corrosion is thought to initiate at coating defects and holidays such that T_i is the same as for black steel; however, propagation rate is low (relatively large T_p)

because of both high resistance between anode and cathode and small cathode surface area (assuming the bottom mat steel, as well as the top, is coated).
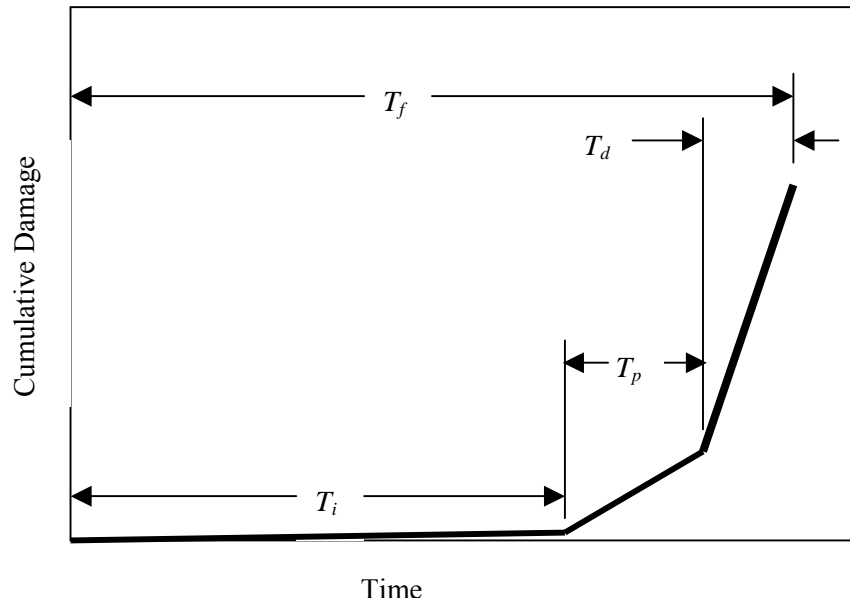
Figure 2. Schematic illustration of the various steps in deterioration of reinforced concrete due to chloride-induced corrosion.

During the past several decades, the approach taken by the Federal Highway Administration (FHWA) and most State Departments of Transportation (DOT) has been to specify epoxy-coated reinforcing steel (ECR) for bridge decks augmented by low water-to-cement ratio (w/c) concrete, possibly with pozzolans or corrosion inhibitors (or both), and concrete covers of 65 mm or more.[12] In Florida coastal waters, ECR has proven ineffective because of higher average temperatures, chlorides, and moisture.[13,14,15,16] Here, practitioners are relying on pozzolans, corrosion inhibitors, and relatively large cover, and are projecting a 75-year life for bridge members in and near the splash zone. Likewise, the methods of life cycle cost analysis (LCCA) are employed to evaluate and compare different materials selection and design alternatives. This approach considers both initial cost and the projected life history of maintenance, repair, and rehabilitation that are required until the design life is reached. These are then evaluated in terms of the time value of money, from which present worth is determined. Comparisons between different options then can be made on a cost-normalized basis.

The above process becomes accelerated if concrete cracks wider than 0.3 mm are present because, in this case, detrimental species, chlorides in particular, and water may have direct access to the reinforcement, irrespective of the depth of cover.[17,18] Here, corrosion resistance relies upon inherent properties of the reinforcement in an electrolyte of pH lower than that of normal pore water.

The mechanism of Cl⁻ intrusion into concrete invariably involves both capillary suction and diffusion; however, for situations in which the depth of the capillary suction

is relatively shallow compared to the reinforcement cover, diffusion alone normally is assumed. Analysis of diffusion is accomplished in terms of Fick's second law,

$$\frac{\partial c(x,t)}{\partial t} = \frac{\partial}{\partial x}\left(D \cdot \frac{\partial c(x,t)}{\partial x}\right), \tag{9}$$

where $c(x,t)$ is the Cl$^-$ concentration at depth x beneath the exposed surface after exposure time t, and D is the diffusion coefficient. As equation 9 is expressed, D is assumed to be independent of concentration. The solution in the one-dimensional case is

$$\frac{c(x,t) - c_o}{c_s - c_o} = 1 - \text{erf}\left(\frac{x}{2\sqrt{D \cdot t}}\right), \tag{10}$$

where

c_o is the initial or background Cl$^-$ concentration in the concrete, and

c_s is the Cl$^-$ concentration at the exposed surface.

To arrive at this solution, assume c_s and D are constant with time, and the diffusion is "Fickian," that is, there are no Cl$^-$ sources or sinks in the concrete. In actuality, c_s increases with exposure time, although Bamforth reported this to reach steady-state after about 6 months for marine exposures.[19] Based on a literature study of marine exposures, values in the range 0.2 to 1.0 percent (concrete weight basis)[1] were reported; however, Howell and Tinnea measured c_s as high as 2.1 percent for an Alaskan viaduct.[20] Factors that affect c_s have been projected to include (1) type of exposure, (2) mix design (cement content, in particular), and (3) curing conditions.[21] Also, the diffusion coefficient that is calculated from equation 10 is termed an effective value, D_{eff}, because it is weighted over the relevant exposure period as a consequence of c_s varying with time, progressive cement hydration, and the possibility of chloride binding, which renders the migration non-Fickian.

By the approach represented by equation 10, $c(x,t)$, c_o, and c_s are measured experimentally (normally by wet chemistry analysis), and D_{eff} is calculated based upon knowledge of reinforcement cover and exposure time. Experimental scatter and error may be minimized by measuring $c(x,t)$ at multiple depths and employing a curve-fitting algorithm to calculate D_{eff}. Also, if D_{eff} is known from one sampling set, then c_{th}, the Cl$^-$ threshold for passive film breakdown and onset of active corrosion, can be determined by measuring $c(x,t)$ at the reinforcement depth (c_{rd}) at the time of corrosion initiation and solving equation 10, recognizing that for this situation, $c_{rd} \approx c_{th}$. In any case, the parameters that affect Cl$^-$ intrusion rate are c_s and D_{eff}, where the former is exposure

---

[1] Numerous methods exist in the literature for reporting the concentration of chlorides in cementitious materials. These include either weight or percent Cl$^-$ in reference to either the concrete or cement. Conversion of the Cl$^-$ amount from a concrete to cement basis or vice versa requires that the cement content be known. In the absence of this information, a cement content can be assumed.

dependent and the latter is a material property (actually, c_s is also sensitive to material composition and microstructure, and D_{eff} is affected by exposure conditions (relative humidity and time of wetness, for example).

Corrosion Control Alternatives

General

Corrosion control options for reinforced concrete structures can be represented in terms of two general categories according to whether they apply to existing Cl⁻ contaminated structures or to new structures. This topic is addressed below in terms of each of these subdivisions.

Existing Structures

The inventory of corrosion-damaged bridge decks in the United States and other countries is such that damage intervention normally transpires only after major repair or rehabilitation (or both) is needed. Rehabilitation includes (1) installation of physical barrier systems such as coatings, sealers, membranes, and overlays to forestall subsequent Cl⁻ ingress, and (2) applying electrochemical methods such as electrochemical chloride extraction (ECE) that revert the concrete to a lesser Cl⁻ contaminated state with enhanced alkalinity in proximity of the reinforcement and cathodic protection for corrosion protection. However, the physical barrier-type repair and rehabilitation methods have no lasting effect if Cl⁻ contaminated or carbonated concrete remains in place. Cathodic protection, in contrast, is the only methodology for which long-term service data are available that has been judged effective for controlling ongoing steel corrosion in Cl⁻ contaminated, atmospheric, or splash zone exposed structures. While the theory and principles of cathodic protection have been known for more than a century, its early application for protecting reinforcing steel in concrete often was not successful because of (1) difficulties in assuring a uniform current density in the high resistivity concrete pore water environment; (2) an absence of adequately performing impressed current anodes; and (3) a lack of understanding and appreciation of cathodic protection technology on the part of transportation maintenance personnel. The first of these difficulties has been overcome largely by proper design and by specifying that anodes be distributed. Concerns regarding the second factor have been reduced by a combination of proper design and the advent of distributed mixed metal oxide-type anodes. Cathodic protection is not necessarily effective in protecting steel exposed at concrete cracks and at spalls in atmospheric applications, but this is probably not an impediment in water or wet soils. This technology cannot, of course, restore structural integrity to cracked or spalled concrete or to embedded steel that has already corroded. Protection criteria normally are based on polarization or depolarization of a prescribed magnitude, typically 100 millivolts (mV).[22] As such, potential need not be reduced to the reversible value for the anodic reaction (as is normally specified for aqueous exposures), and corrosion rate may not be reduced to nil but simply to a relatively low value. Protection may result, not only from the polarization but also from electromigration of Cl⁻ away from the reinforcement

and resultant steel repassivation by this and by generating OH⁻ in conjunction with the cathodic reaction.

ECE is a relatively new technology for which long-term service data are limited.[23,24] This method employs a temporary anode that is operated at current density orders of magnitude higher than for cathodic protection, such that anions, including chlorides, electromigrate away from the embedded steel cathode. Repassivation can then occur, similar to what was discussed above in conjunction with cathodic protection, although this occurs in a shorter period of time (1–2 weeks to several months). Not all chlorides are removed, but sufficient amounts are displaced from the steel-concrete interface. This technology's effectiveness probably rests as much, or more, on hydroxide generation at the steel and an associated decrease in [Cl⁻]/[OH⁻] as on chloride removal or redistribution.

New Structures

Factors to be considered in designing corrosion control of new reinforced concrete structures include (1) embedded steel surface protection, (2) concrete mix design, (3) structural design considerations, (4) concrete surface modification, (5) cathodic prevention, and (6) corrosion-resistant reinforcement (CRR). The first of these (embedded steel surface protection) exemplified by epoxy-coated reinforcement. These coatings permit movement of moisture to the steel surface but restrict oxygen penetration such that a necessary reactant at cathodic sites (see equation 3) is excluded. ECR has been employed in bridge decks for almost 30 years with generally good results reported for this application. However, cracking and spalling of bridge substructure concrete components from corrosion of ECR occurred for splash and near splash zone locations of the overseas highway to Key West, FL, only 7 years after construction.[17,18] Different opinions have been provided as explanations for this, with some considering that the semitropical splash zone is particularly harsh with regard to corrosion at coating defects and undercoating corrosion, and that this same type of deterioration may also occur with more modest exposures but simply at a reduced rate.[19] Presently, there is concern that ECR may not provide the target 75-year design life that is now specified for reinforced concrete bridge decks without some maintenance.

Historically, black bar with a corrosion-resistant metal or alloy cladding has been considered for reinforcing concrete undergoing severe exposure. Of the options that have been studied, galvanized reinforcing steel is the most prominent and has been employed in concrete to a limited extent. Here, a relatively thin zinc surface layer is applied by either hot dipping or electro-deposition. This methodology relies on a relatively low corrosion rate for zinc and its potential for being active to the substrate steel, thereby providing galvanic cathodic protection at defects and penetrations. However, the results of research programs have been mixed, probably as a consequence of zinc being amphoteric, such that passivating corrosion products apparently do not form at pH > 13.3.[25,26] Noble metal claddings such as copper, nickel, and stainless steel have historically been investigated but have not been used extensively due to initial cost considerations. Renewed interest has recently focused upon the utility of reinforcements

of this type, however, because of their potential for providing greater corrosion resistance than black bar alone but at a reduced cost compared to situations where the entire bar cross section is corrosion resistant. This, coupled with development of unique manufacturing methods, has made available stainless clad bars in the price range $1.08–$1.65/kg.

Concrete mix design modifications involve such factors as (1) reduced w/c, including use of water-reducing admixtures or superplastizers; (2) type of cement; (3) permeability reducing admixtures such as fly ash, silica fume, and blast furnace slag; and (4) corrosion inhibiting admixtures. In effect, options 1 and 3 reduce D_{eff}, whereas options 2 and 4 can function by elevating c_{th}.

Structural design aspects of corrosion control involve factors such as configurational (geometrical) considerations that minimize or, if possible, eliminate exposure to corrosives. For example, Florida DOT now requires, wherever possible, elevation of bridge superstructures to a minimum of 4 meters (m) above mean high tide. Of particular importance is also depth of concrete cover over the reinforcing steel. The significance of this parameter is apparent from equation 10.

Coatings, sealers, and membranes (physical methods) also can be specified for new structures. However, it is generally accepted that such treatments will not provide a 75-year design life unless they are supplemented by other options, such as use of impermeable concrete and large cover.

Cathodic prevention is, in effect, identical to cathodic protection, except that it is applied to new, Cl⁻-free structures for which current demand is less than for Cl⁻ contaminated ones. In addition, the objective here is not to reduce corrosion rate itself (because the reinforcement is passive), but instead to establish a potential gradient that opposes the inward diffusional migration of anions, specifically chlorides. In this regard, the approach functions similarly to ECE, except that, instead of removing chlorides, it retards their entry.

Historically, the added initial cost of CRR, such as stainless steel, has largely precluded it from being competitive for concrete construction. However, with the advent of LCCA and the FHWA requirement in 1995 that bridge projects that cost more than $25 million have a 100-year design life, including reinforcements of this type has become a more viable option. However, although there have been research studies and scientific and engineering literature reviews pertaining to CRR in concrete and simulated concrete environments, the long-term corrosion performance of such materials in bridge applications still cannot be projected confidently.[27,28,29,30] The issue is complicated by the fact that there are a variety of CCR choices that cover a range of manufacturing processes, cost, and corrosion performance. This, combined with the very real need to reduce the social and economic impact of bridge maintenance costs, has resulted in a need for additional research. This critical review of CRR performance in concrete has been prepared as a prelude to further FHWA-sponsored research on this topic.

CORROSION-RESISTANT REINFORCING STEEL

General

Within the present context, CRR is defined as reinforcing steel that exhibits improved corrosion behavior in chloride contaminated concrete compared to conventional bare, black steel.[31] Accordingly, primary emphasis is placed on stainless steels and modified stainless steels, including propriety alloys and stainless steel clad bars that are presently available.

Stainless Steels

General

The term stainless steel generically refers to iron base alloys with a minimum of 12 weight percent (w/o) Cr. At this Cr concentration, a passive film self-forms on air and water exposure. In addition, common alloying elements include Ni, Mo, N, Ti, and perhaps others. Except for martensitic stainless steels, carbon is an impurity. Stainless steels that are being considered for reinforcing concrete are of either a ferritic, austenitic, or duplex (ferrite plus austenite) microstructure according to the phase(s) present, which, in turn, is determined by composition. As such, Cr is a ferrite (bcc) stabilizer, whereas Ni stabilizes austenite (fcc). Other classes of stainless steel are martensitic (noted above), super-ferritic, super-austenitic, and precipitation-hardenable. For various reasons, including excessive strength (martensitic and precipitation-hardenable), poor corrosion resistance (martensitic), and higher than necessary alloying element concentrations and, hence, cost (super-ferritic and super-austenitic), the super-ferritic, super-austenitic, and precipitation-hardenable classes are not considered viable reinforcement candidates.

Ferritic stainless steels typically have less than 17 w/o Cr and little or no Ni. For austenitics, Cr is 18–20 w/o, and Ni is 8–10 w/o. Other alloying elements also may be present (for example, 2 and 3 w/o Mo for American Iron and Steel Institute (AISI) Types 316 and 317, respectively). Ferritic-austenitic stainless steels, termed duplexes, contain 22–28 w/o Cr and 4–8 w/o Ni. This yields a microstructure comprised of both ferrite and austenite, typically at a 50–50 ratio. The super-ferritics typically contain ~25–30 w/o Cr and <4 w/o Ni and the super-austenitics ~20 w/o Cr, and 18–25 w/o Ni.

Stainless steel has been employed as concrete reinforcement in Canada, Denmark, Germany, Italy, Japan, Mexico, South Africa, the United States, and the United Kingdom. While this reinforcement has been used throughout some structures, stainless steel has more generally been limited to construction joints or critical gaps between columns and decks.

Relevant Material Properties

The relevant material properties for reinforcing corrosion-resistant or conventional steel are mechanical, corrosion, weldability, thermal, magnetic, and economic. Mechanical properties are addressed by applicable standards and design codes, whereas the other properties are more subjective and addressed by the designer in conjunction with materials selection considerations.

Corrosion Behavior of Stainless Steels

Although the literature addressing corrosion of stainless steels is voluminous, it pertains largely to acid and seawater rather than highly alkaline applications. Much emphasis has been placed on identifying the alloy (of which there are hundreds) that provides adequate corrosion resistance for the application in question (in the present context, reinforced concrete bridges) at minimal cost.

The most common forms of corrosion for stainless steels are localized (pitting, crevice, and intergranular) and environmental cracking. Of these, pitting is the most relevant form for reinforcing steel in concrete structures. Resistance to pitting attack historically has been characterized by any one of several parameters, including (1) critical pitting potential, ϕ_{crit}, (2) critical pitting temperature (CPT) and (3) the pitting resistance equivalent (PRE or, alternatively, pitting resistance equivalent number (PREN)). The first of these, ϕ_{crit}, is defined as the least positive potential for which pitting occurs. This is illustrated schematically in figure 3 for the case of an electrode such as stainless steel exposed to aqueous solutions with and without Cl⁻. Here, the two anodic polarization curves are characterized by passivity and a relatively low, potential independent current density regime at negative potentials that transitions at more positive potentials to high current densities. The passive current density is lower, and the transition to higher current density occurs at a more positive potential in the absence of Cl⁻. This current density increase is a consequence of O_2 evolution, not corrosion. With Cl⁻, however, the current density transition results from the onset of pitting. Figure 4 shows schematically how the anodic polarization curve and ϕ_{crit} are affected by temperature, Cl⁻ concentration, and alloy composition. Thus, the passive domain is compromised by increasing temperature and Cl⁻ concentration, and expanded by increased Mo concentration.
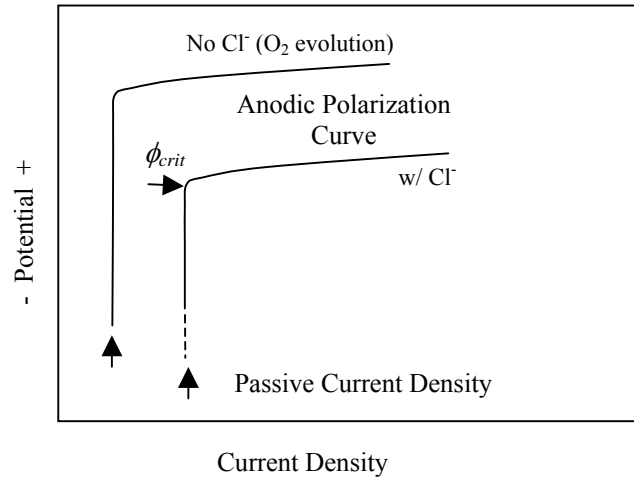
Figure 3. Schematic polarization curve for stainless steel in an aqueous solution with and without Cl⁻.
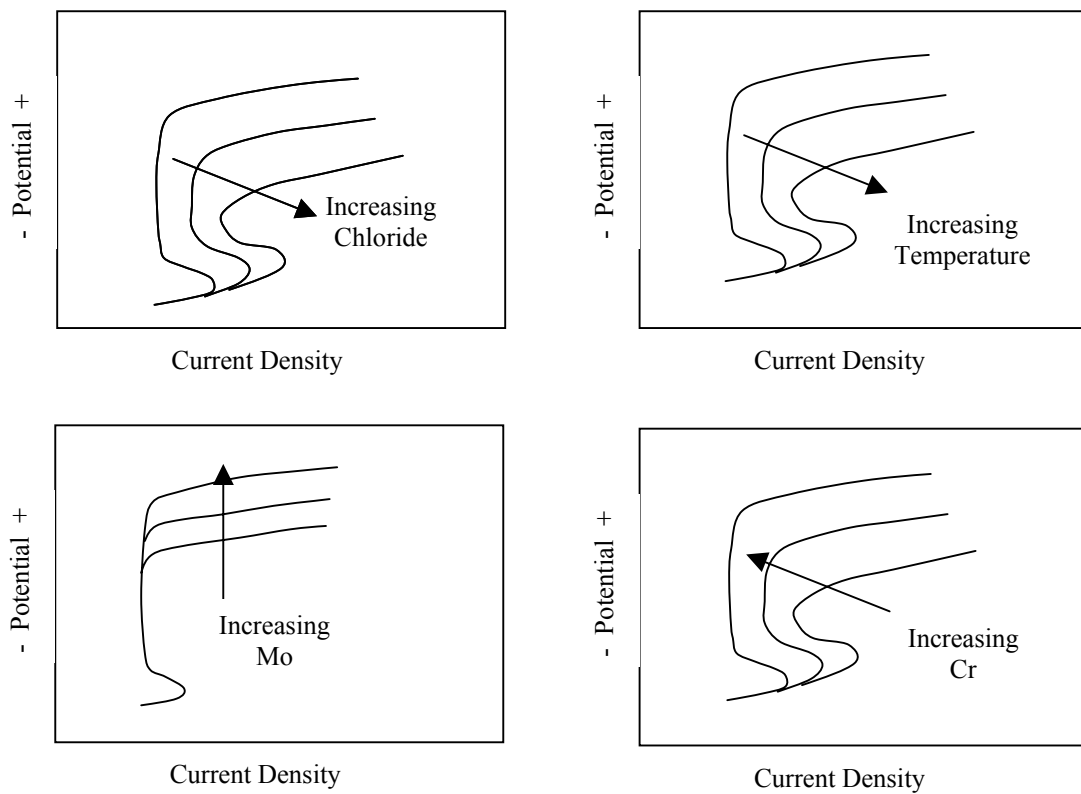

Figure 4. Schematic anodic polarization curves illustrating dependence of the anodic polarization curve for stainless steels on temperature, Cl⁻ concentration, and alloy composition.

A critical aspect of pitting resistance is the magnitude of the difference between the critical pitting potential (ϕ_{crit}) and the corrosion potential (ϕ_{corr}), as illustrated schematically by figure 5. Thus, pitting should not occur in situations where ϕ_{corr} remains negative to ϕ_{crit} and vice versa. Table 1 illustrates this by comparing these two parameters based on 4.25 years' exposure of various alloys in seawater, and figure 6 plots $\phi_{crit} - \phi_{corr}$ versus weight loss, where the latter parameter indicates the extent of pitting corrosion.[32]

The finding that resistance to pitting decreases with increasing temperature (figure 4) is the basis for defining this resistance in terms of a critical temperature; that is, a temperature below which the passive film does not break down locally, and above which it does. This temperature is determined experimentally by polarizing the metal or alloy in question at a constant potential more positive than ϕ_{corr} and progressively increasing temperature. The onset of a current density increase then defines the CPT.
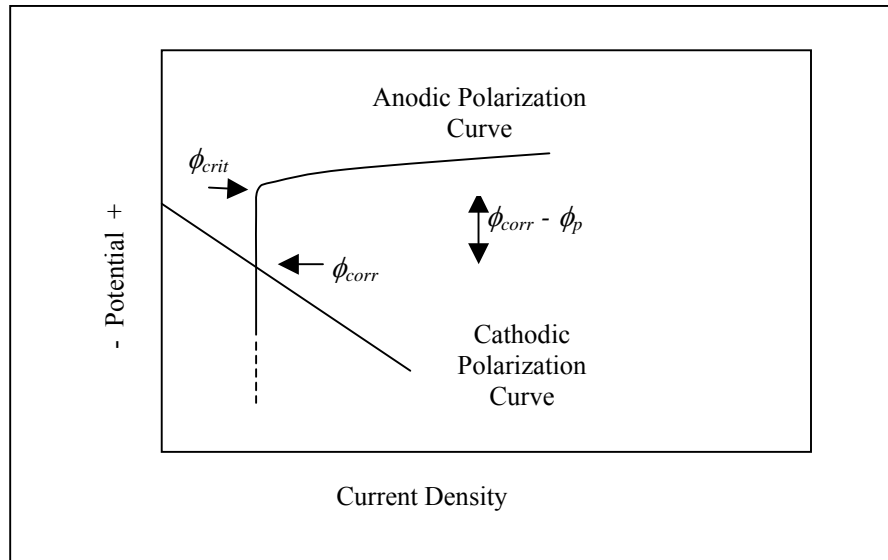
Figure 5. Schematic illustration of the ϕ_{crit} and ϕ_{corr} parameters.

Table 1. Comparison of ϕ_{crit} and ϕ_{corr} for selected materials.

Alloy Designation	ϕ_{crit}, V_{SCE}	Range for ϕ_{corr}, V_{SCE}
Type 430 SS	-0.130	-0.310 to 0.230
Type 304 SS	-0.020	-0.140 to 0.280
Type 316 SS	0.100	0.090 to 0.385
Carpenter 20 Cb™	0.05	0.120 to 0.520
Incoloy 825™	0.525	0.180 to 0.530
Hastelloy C™	>0.900	0.530

SS: Stainless steel.

Although the difference between ϕ_{crit} and ϕ_{corr} and the CPT indicate resistance to pitting, as explained above, the PRE/PREN more often is employed for materials selection purposes for austenitic and duplex stainless steels. This parameter is calculated from the expression

$$PRE(PREN) = \%\cdot Cr + 3.3 \cdot \%Mo + A \cdot \%N, \qquad (11)$$

where A typically ranges from 6 to 30, with a value of 16 being commonly employed for duplex stainless steels and 30 for austenitics. As such, the PRE/PREN is based solely on composition of three alloying elements. Also, note the relatively strong influence of N, followed by Mo. PRE values in excess of 40 generally are considered necessary to avoid pitting and crevice corrosion in ambient seawater. A lesser value should suffice for stainless steels in concrete because of the relatively high pore water pH and the corrosion inhibiting role of OH⁻, as discussed above.
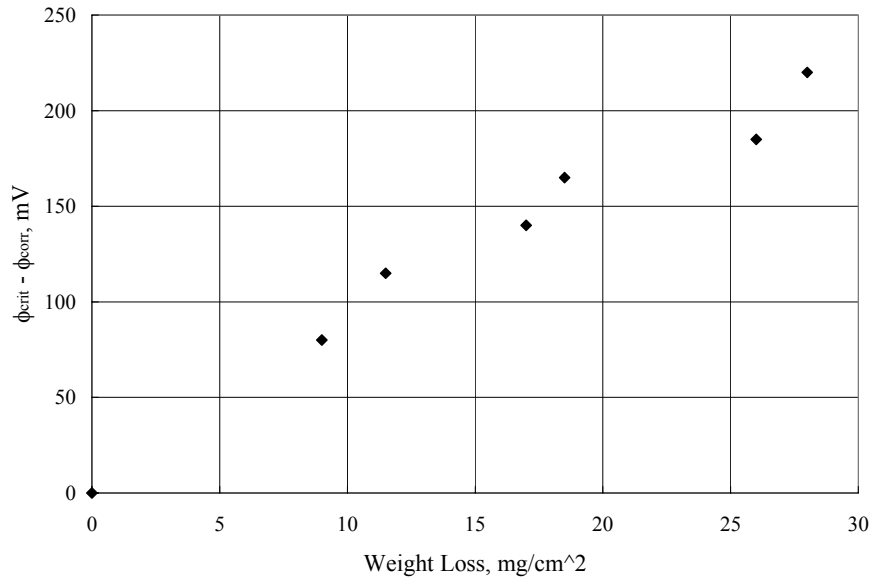
Figure 6. Seawater exposure data illustrating a correlation between $\phi_{crit} - \phi_{corr}$ and weight loss due to pitting.

Table 2 lists PRE/PREN values for several common stainless steels. Although the PRE/PREN provides a quantitative measure of performance, it does not consider the effect of other alloying elements, impurities, and microstructure, all of which can be important. In addition, equation 11 has evolved from a wide base of experience in acid processing fluid exposures and not for steel in concrete. While the general qualitative nature of the expression is expected to apply in concrete as well, the coefficients may be different.

Table 2. PRE/PREN for some common stainless steels.

Stainless Alloy	PRE/PREN (A = 16)
Type 430	17
Type 304	18
Type 316	24
Type 316LN	26

As noted above, the critical pitting potential increases with increasing pH because OH⁻ serves as a passivator. Figure 7 provides a schematic illustration of the combined pH and Cl⁻ effect, such that a surface is generated corresponding to ϕ_{crit}. With increasing PRE/PREN, this surface of ϕ_{crit} values is displaced toward more positive potentials.
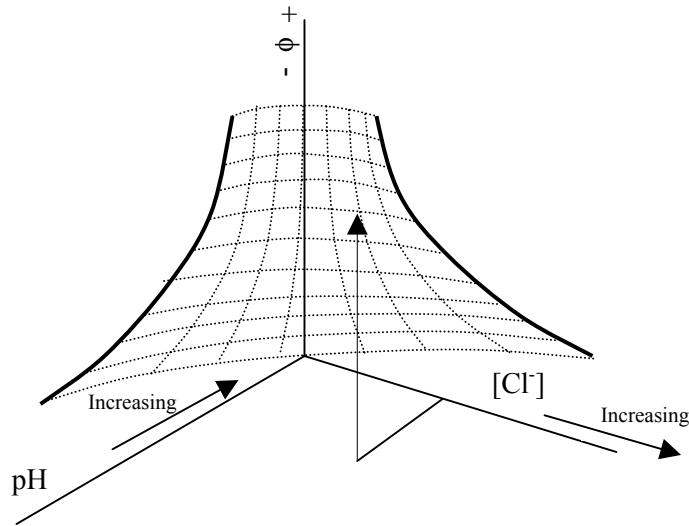
Figure 7. Schematic illustration of the combined effect of pH and Cl⁻ on ϕ_{crit}.

Pitting Mechanism

Theories of passivity fall into two general categories, one based on adsorption and the other on presence of a thin oxide film. Pitting in the former case arises as detrimental or activator species, such as Cl⁻, compete with O_2 or OH⁻ at specific surface sites. By the oxide film theory, detrimental species become incorporated into the passive film, leading to its local dissolution or to development of conductive paths. Once initiated, pits propagate auto-catalytically according to the generalized reaction,

$$M^{+n} + nH_2O + nCl^- \rightarrow M(OH)_n + nHCl, \qquad (12)$$

resulting in acidification of the active region and corrosion at an accelerated rate (M^{+n} and M are the ionic and metallic forms of the corroding metal). As evidence of this process, acidic pH values are routinely measured at actively corroding sites on

22

reinforcing steel upon breaking open Cl⁻ contaminated concrete irrespective of the alkaline pore water.[1]

Particularly noteworthy is the pitting mechanism proposed by Galvele[i,ii] and Muller and Gavele.[iii] This is predicated on the anodic process (equation 2) occurring at the base of a cylindrical pit or similar geometrical feature and supported by an Na salt containing electrolyte followed by hydrolysis (equation 12). Pit stability requires maintaining a critical [H⁺], designated pH_{crit}. This was assumed as the value at which the oxide (passive) film is in equilibrium with dilute metal ions in solution based on the reaction

$$Me(OH)_{n(s)} \rightarrow Me^{n+}_{(aq)} + nOH^-_{(aq)}, \tag{13}$$

where

$$K_s = \left[Me^{n+}\right] \cdot \left[OH^-\right]^n, \tag{14}$$

with K_s being the solubility product. The model demonstrated that a stable pH_{crit} resulted when the product of pit depth and current density achieved a critical value. Thus, both generating Me^{+n} via the anodic reaction and confining the H^+ hydrolysis product (as occurs with increasing pit depth or surface irregularities and an associated restriction on outward diffusion and electromigration of cations), facilitate pitting. s

Galvele reasoned further that ϕ_{crit} is the most negative potential at which pH_{crit} can be maintained at the metal-solution interface. This was expressed analytically as

$$\phi_{crit} = \phi_{corr} + \eta + \phi_{inh} + \phi, \tag{15}$$

where η if magnitude of the positive (anodic) polarization from ϕ_{corr}, ϕ_{inh} is the potential shift associated with presence of any inhibitor, and ϕ is the potential gradient in the pit.

The concept that the criterion for pit initiation is that the product of current density (i_c) and surface feature depth (x) achieve a critical value has important implications for stainless steels in corrosive service, including those of reinforcing steel in concrete. This arises because surface treatments such as thermal-mechanical processing, welding, and pickling all affect surface roughness. Accordingly, pitting susceptibility, as reflected by ϕ_{crit} or by CPT (although not by PRE/PREN) should vary in proportion to surface roughness that arises from a particular processing or treatment.

EXPERIMENTAL METHODS AND FINDINGS

Background

Experimental techniques that historically have been employed to investigate corrosion phenomena associated with reinforcing steel in concrete (both plain carbon and corrosion resistant), have involved the following categories:

1. Laboratory studies in synthetic aqueous solutions.
2. Laboratory studies with cementiteous embedments.
3. Test yard and field exposure of concrete specimens.
4. Actual structures.

Typically, selecting one method over another recognizes a tradeoff between time and cost versus realistic simulation of actual service with each of these three factors increasing from 1–4. Also at issue is whether a specific method provides design relevant data (time-to-corrosion (t_i, see figure 2) and Cl$^-$ threshold, for example) or simply information that facilitates ranking of materials. Thus, experiments in category 1 tend to focus on determining the interrelationship between ϕ_{crit}, pH, and Cl$^-$ concentration (see figure 7) using aqueous solutions that simulate pore water and employing either potentiodynamic anodic polarization or potentiostatic polarization to a relatively positive potential (or both). Methods in categories 2 and 3 use either mortar or concrete-coated specimens, often with relatively high w/c's, low cover, and admixed Cl$^-$ and measurement of corrosion potential or corrosion rate by polarization resistance or macrocell current determinations (or both). Time-to-corrosion can also be determined. Category 4 does not represent a specific experimental technique but rather a demonstration or prototype structure. Studies in each of these four areas are reviewed and discussed below.

Laboratory Studies in Synthetic Aqueous Solutions

McDonald et al. performed a comprehensive screening program on a wide variety of CRRs, including stainless steels, as a prelude to testing yard-type exposures.[33] This involved successive 1.75 hours wet–4.25 hours dry exposure in NaCl solutions of pH 7 and 13 of bars that had been bent about a mandrel of diameter 4 times that of the bars. The pH 7 solution simulated preconstruction atmospheric exposure or conditions within a concrete crack; the pH 13 solution simulated concrete pore water. Table 3 lists polarization resistance (PR) and corrosion rate (CR) results for the pH 7 case, and figure 8 shows the corrosion rate data graphically. These indicate that corrosion rate for the stainless steels varied by as much as an order of magnitude, with most data being in the range 0.1–1.0 mille-Amps per meter squared, depending on the specific alloy, or from 2–3 orders of magnitude less than for plain carbon steel.

Table 3. Polarization resistance and corrosion rate data for CRR candidates in accelerated screening tests at pH 7.

Reinforcement Type	Bar Cond***	pH 7 + 3 w/o NaCl					
		28 Days		56 Days		90 Days	
		PR, Ohm·m^2	CR, mA/m^{2*}	PR, Ohm·m^2	CR, mA/m^{2*}	PR, Ohm·m^2	CR, mA/m^{2*}
Plain Carbon (Black)	As-Recorded	0.05	520	0.14	186	0.05	520
	Hole	0.04	650	0.05	520	0.04	650
Type 304	As-Recorded	100.40	0.26	52.42	0.50	90.96	0.29
	Hole	84.87	0.31	133.50	0.19	121.47	0.21
Type 304U**	As-Recorded	12.57	2.07	11.88	2.19	–	–
	Hole	6.03	4.31	9.70	2.68	9.17	2.84
Type 304N	As-Recorded	43.10	0.60	59.10	0.44	76.6	0.34
	Hole	52.70	0.49	67.63	0.38	124.88	0.21
Type 304 Clad	As-Recorded	93.41	0.28	81.21	0.32	186.77	0.14
	Hole	10.60	2.45	12.33	2.11	12.73	2.04
	Abrade	54.38	0.48	49.57	0.52	90.69	0.29
Nitronic 33™	As-Recorded	38.53	0.67	57.11	0.46	97.63	0.27
	Hole	289.30	0.09	89.73	0.29	442.4	0.06
Type 316	As-Recorded	48.67	0.53	21.57	1.21	29.78	0.87
	Hole	56.36	0.46	135.20	0.19	130.5	0.20
Type 317LN	As-Recorded	107.90	0.24	131.20	0.20	179.1	0.15
	Hole	37.20	0.70	93.88	0.28	168.34	0.15
Type XM19	As-Recorded	133.90	0.19	115.40	0.23	350	0.07
	Hole	125.70	0.21	248.20	0.10	466.3	0.06

*   Calculated as CR = 0.026*1000/PR.
**   European source.
***   Six mm diameter hole (through cladding in the case of clad bars).

Similarly, table 4 and figure 9 show comparable data for a 0.30N KOH+0.05N NaOH solution (pH ≈ 13). Salt concentration as NaCl for each of 3 successive 56 day test periods was 3, 9, and 15 w/o, respectively. These yielded Cl⁻-OH⁻ ratios of 1.5, 4.5, and 7.5, respectively. The more corrosion-resistant materials were not tested in the higher pH solution. In all cases, corrosion rates were lower at pH 13 than at pH 7 by an amount that approached 1 order of magnitude.

As an alternative approach, Hurley and Scully performed potentiostatic exposures at potentials as high as +200 mV$_{SCE}$ on Types 304 and 316 stainless steel reinforcements in a saturated Ca(OH)$_2$ solution with incremental Cl⁻ as NaCl additions.[36] The threshold

concentration, c_{th}, represented as [Cl$^-$]/[OH$^-$] (molar basis), was related to a current density increase. Figure 10 shows their results as a plot of the [Cl$^-$]/[OH$^-$] molar threshold ratio as a function of potential.
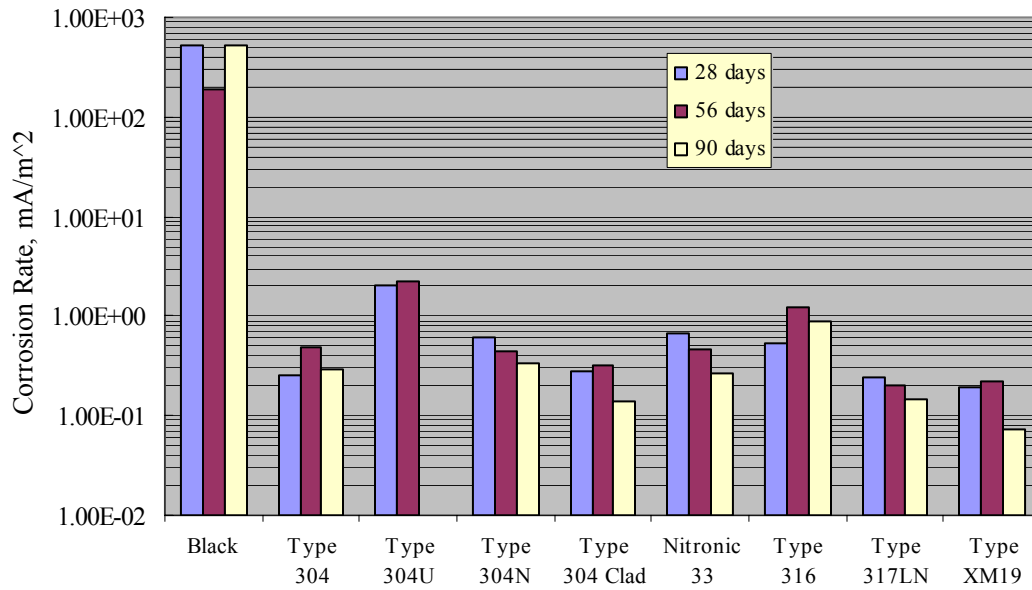

Figure 8. Graphical representation of accelerated screening test data at pH 7.

Table 4. Polarization resistance and corrosion rate data for CRR candidates in accelerated screening tests at pH 13.

Reinforcement Type	Bar Cond.**	pH 13 + NaCl					
		First 56 Days		Second 56 Days		Third 56 Days	
		PR, Ohm·m^2	CR, mA/m^2*	PR, Ohm·m^2	CR, mA/m^2*	PR, Ohm·m^2	CR, mA/m^2*
Plain Carbon (Black)	As-Recorded	1.58	16	0.31	84	0.25	104
	Hole	0.77	34	0.37	70	0.33	79
Type 304	As-Recorded	60.60	0.43	147.90	0.18	–	–
	Hole	40.31	0.65	121.70	0.21	–	–
Type 304 Clad	As-Recorded	68.91	0.38	32.67	0.80	15.26	1.70
	Hole	231.20	0.11	11.75	2.21	-	-
	Abrade	68.33	0.38	–	–	67.8	0.38
Nitronic 33	As-Recorded	108.90	0.24	194.10	0.13	86.12	0.30
	Hole	–	–	54.60	0.48	222.4	0.12
Type 316	As-Recorded	66.37	0.39	96.10	0.27	–	–
	Hole	95.60	0.27	116.90	0.22	–	–

* Calculated as CR = 0.026*1000/PR.
** Six mm diameter hole (through cladding in the case of clad bars).

These authors also reported corrosion potential for various reinforcements based on tests in simulated pore water solutions and in Cl⁻ contaminated concrete, as shown in figure 10, and reasoned that the +200 mV$_{SCE}$ control potential (figure 11) was an upper limit that should not be exceeded in service. As such, the thresholds at +200 mV$_{SCE}$ were projected as being conservative.

Comparable results were obtained by Bertolini et al. based upon both potentiodynamic polarization scans and potentiostatic tests at +200 mV$_{SCE}$ in solutions that simulated both alkaline and carbonated pore water.[37] Figure 12 reports their results as a listing of critical Cl⁻ concentration for the different alloys that were investigated. A correspondence between c_{th} and PRE/PREN is apparent, with the exception of the low carbon Type 304 and 316 stainless steels, for which relatively low thresholds are apparent. The reason for this is unclear.
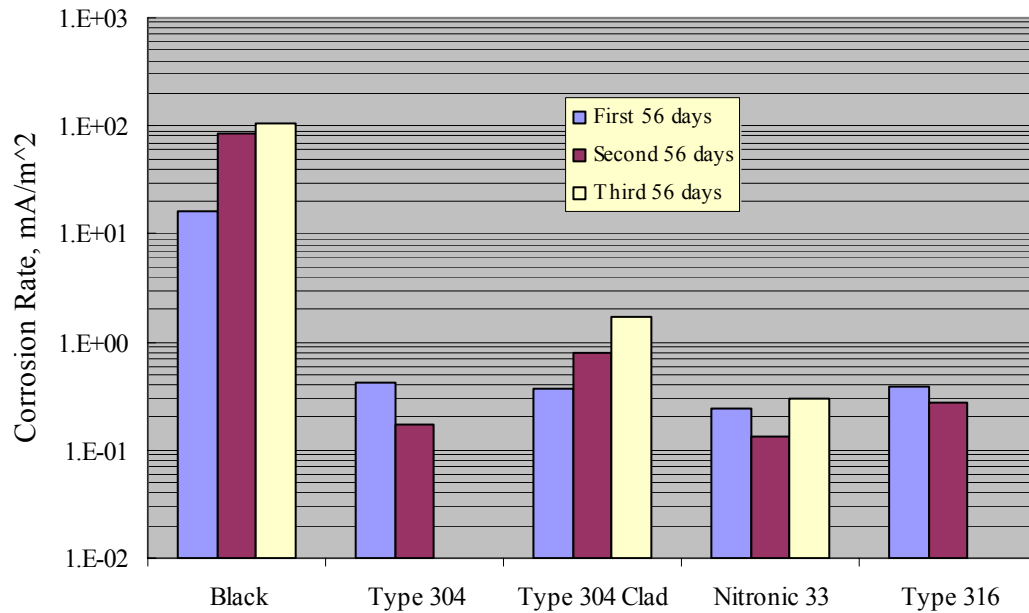
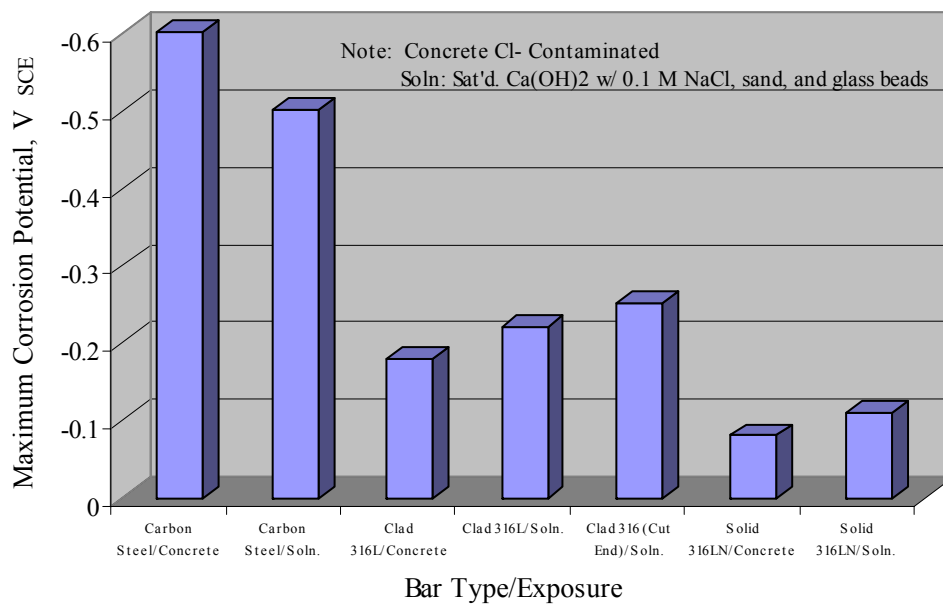Figure 9. Graphical representation of accelerated screening test data at pH 13.

Figure 10. Most positive corrosion potential for different alloys in solution and in concrete.
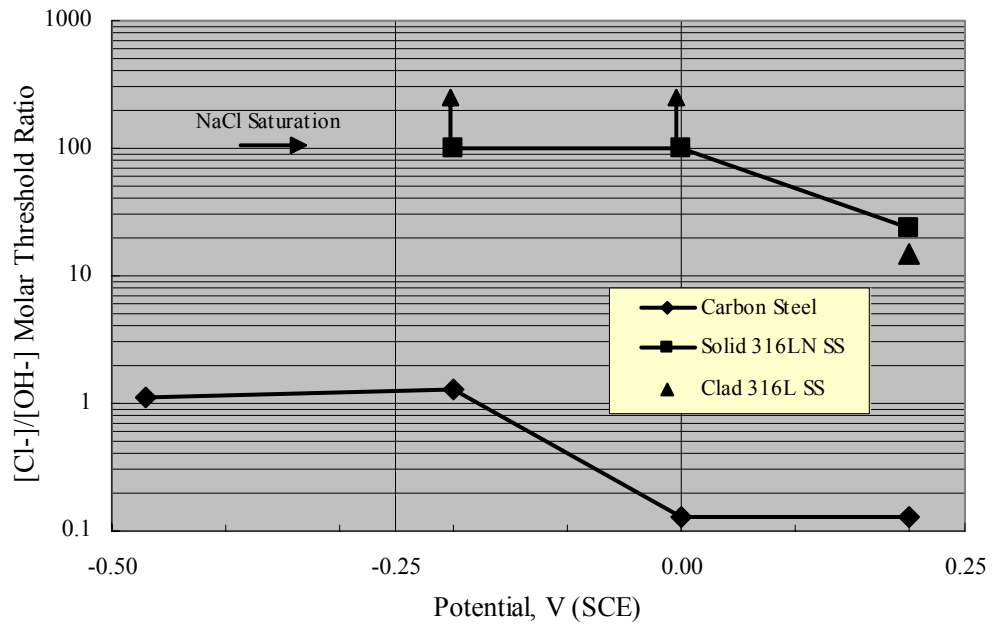
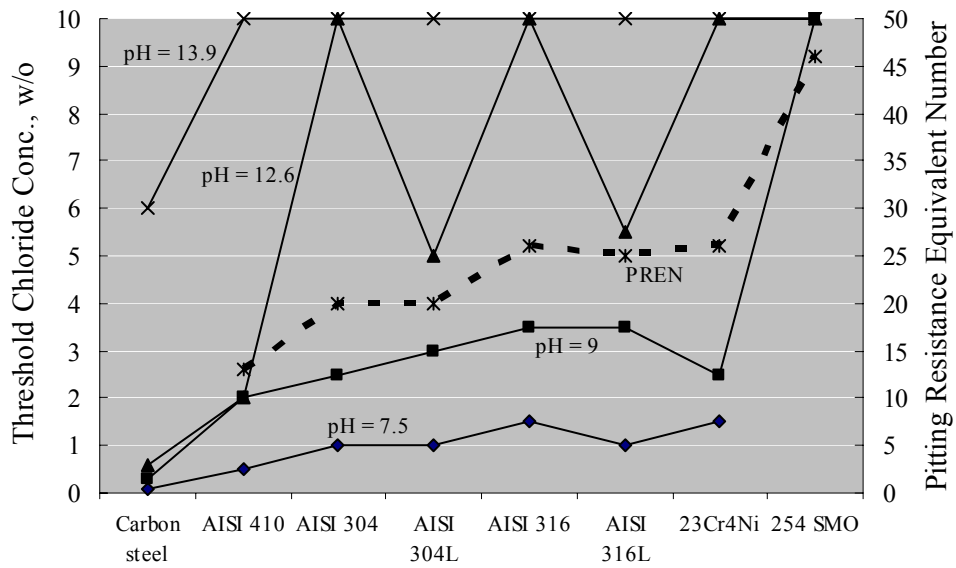Figure 11. Threshold Cl⁻-OH⁻ ratio as a function of potential for stainless and carbon steels.

Figure 12. Threshold Cl⁻ concentration for different reinforcement types in aqueous solutions of different pH.

Laboratory Studies with Cementitious Embedments

Sorensen et al. performed potentiostatic exposures at 0 to +200 mV$_{SCE}$ using mortar prisms with Type 304 and 316 reinforcement and 0–8 percent admixed Cl⁻ exposed in saturated Ca(OH)$_2$ solution with 1 M NaCl.[38] Figure 13 shows the results for Type 304 stainless, both welded and unwelded, as a plot of anodic current density versus admixed Cl⁻ concentration. The passive current density was in the range 10^{-1}–10^{-2} mA/m^2 for the unwelded stainless, or about 1 order of magnitude less than in aqueous solutions (see figures 8 and 9). The greater susceptibility of welded reinforcement to corrosion was attributed to air voids being entrapped at the irregular weld profile and to surface oxides. Enhanced surface roughness may also have been a factor.[39] Figure 14 presents data for these same specimens in a time-to-corrosion format.
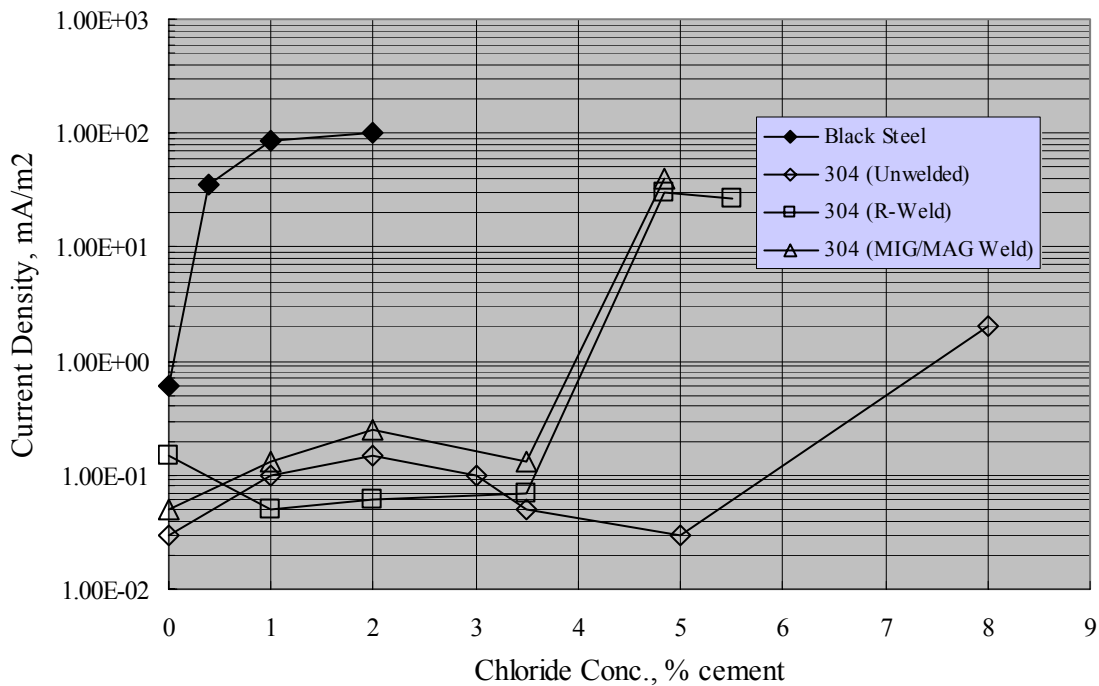

Figure 13. Current density as a function of admixed chloride concentration for mortar specimens potentiostatically polarized at 0 mV$_{SCE}$.

Reduced performance for welded versus unwelded stainless steel was confirmed by experiments by Nürnberger et al., who performed preliminary potentiodynamic and subsequent, longer term potentiostatic tests upon both carbonated and uncarbonated mortar-coated austenitic and ferritic stainless steel specimens (welded and unwelded) as a function of admixed Cl⁻ concentration.[39]   Figure 15 shows pitting potential data for their unwelded bars, including results for carbon steel specimens.
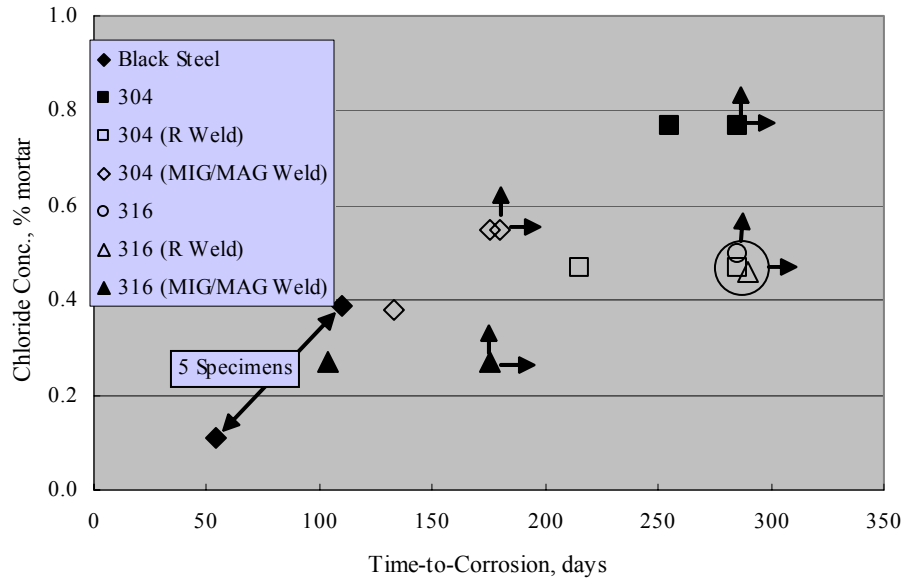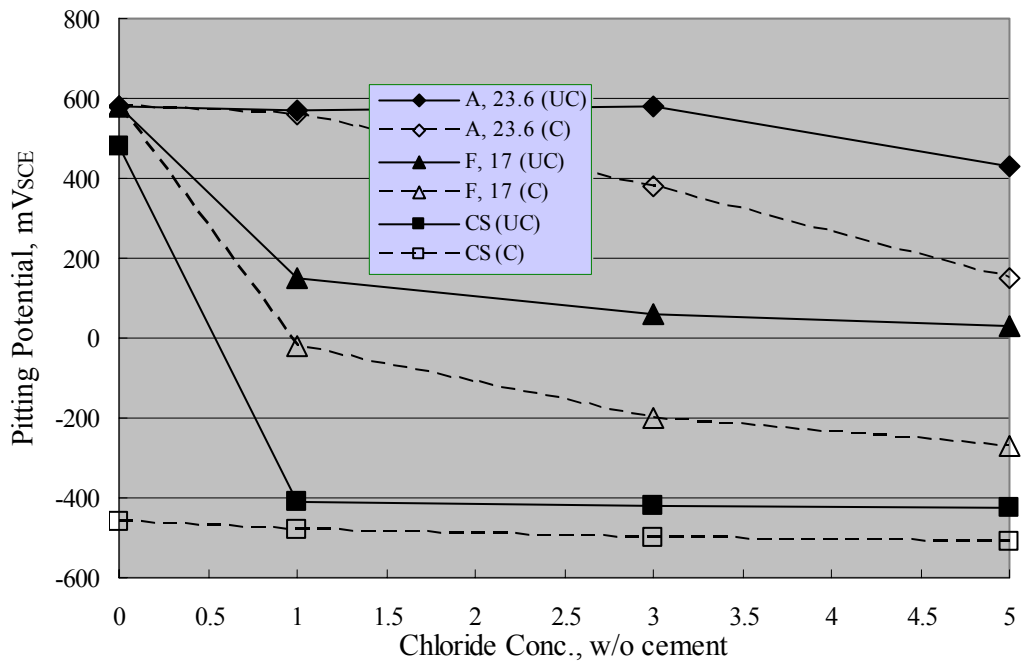
Figure 14. Time-to-corrosion as a function of admixed Cl⁻ concentration.

A = Austenitic
F = Ferritic
CS = Carbon Steel

Figure 15. Critical pitting potential as a function of admixed Cl⁻ concentration for stainless and carbon steel specimens in both carbonated (C) and uncarbonated (UC) mortar. The number in the caption indicates the PREN for each alloy.

Likewise, figure 16 compares these results with those for the welded condition. The trend is one where welding caused a relatively large reduction in ϕ_{crit} for the austenitic material but did not significantly impair performance for the ferritic or carbon steel specimens. This distinction presumably was a consequence of pitting susceptibility being relatively high in the ferritic and carbon steel, irrespective of whether or not these were welded.
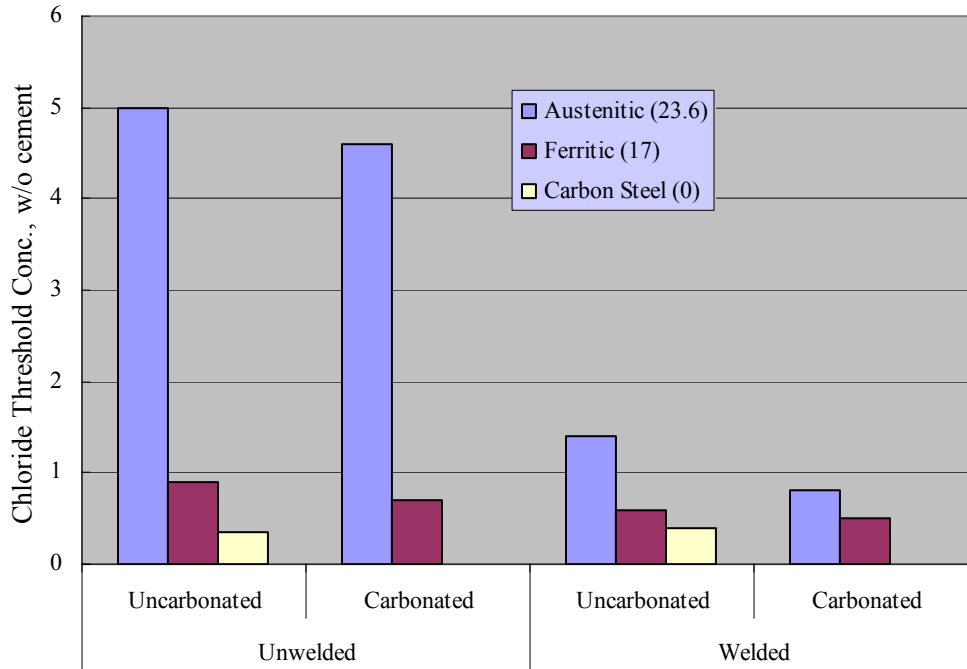

Figure 16. Comparison of c_{th} for welded and unwelded stainless and carbon steel specimens in carbonated and uncarbonated mortar. The number in the caption is the PREN. Where no carbon steel data are indicated, c_{th} was zero.

Figure 17 attempts to interrelate c_{th} data as reported by Sorensen et al. on a w/o cement basis for mortar specimens to $[Cl^-]/[OH^-]$ assuming a 2:1 sand-to-cement ratio, 10 percent pore water, and OH^- activity coefficient 0.7.[42] Also provided is the range of these two parameters (c_{th} and $[Cl^-]/[OH^-]$) that has been reported historically for carbon steel in aqueous solutions or mortars (or both). The fact that the Sorensen et al. data include multiple values for the same material reflects the fact that different constant potentials were employed and c_{th} decreased as potential was made more positive. The data suggest that c_{th} for the stainless steel averaged about one order of magnitude greater than for carbon steel on a w/o cement basis, and from 1–2 orders of magnitude greater in terms of $[Cl^-]/[OH^-]$.
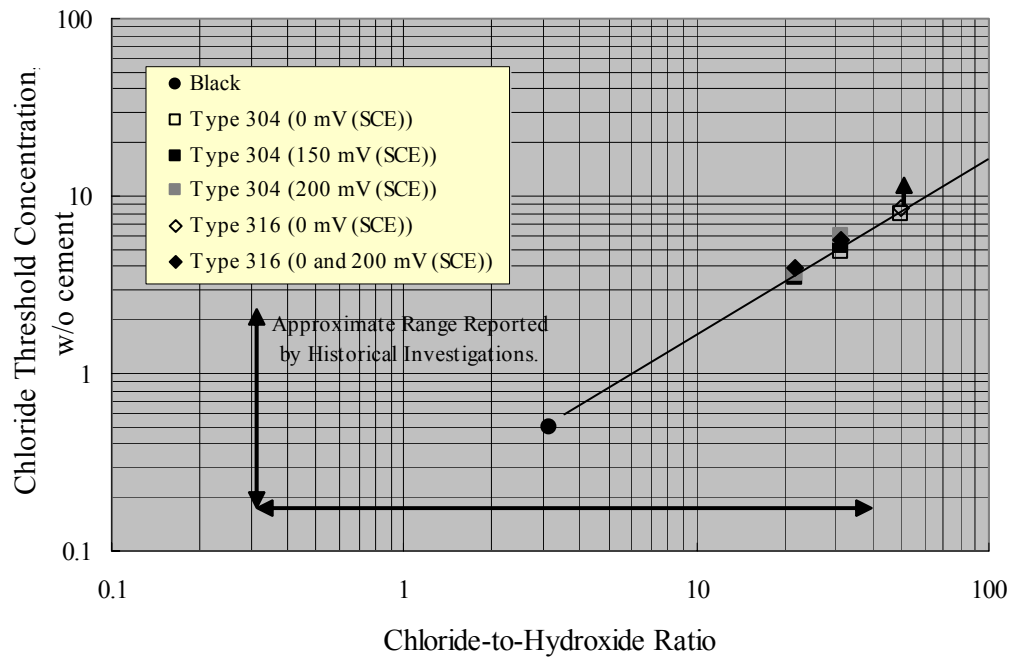
Figure 17. Attempted cross correlation of Cl⁻ threshold on a cement w/o and on a [Cl⁻]/[OH⁻] basis.

Test Yard-Type Exposures

Exposures in this category tend to span the gap between aqueous solution laboratory test cell experiments and actual field service structures. The accelerating features typically include relatively high w/c, low concrete cover, and frequent application of a concentrated salt solution under successive wetting and drying conditions.

Treadaway[40] and Treadaway et al.[41] exposed concrete prisms reinforced with carbon steel, Types 405 and 430 (ferritic) stainless steels, and Types 304, 315, and 316 stainless steels outdoors in the United Kingdom for 10 years. Two mix designs were employed, one with an 8:1 aggregate:cement ratio, cement content 220 kg/m³, and w/c 0.75, and the second with parameters of 6:1, 290 kg/m³, and 0.60, respectively. Concrete cover was either 10 or 20 mm. Admixed Cl⁻ concentration was as high as 3.2 percent (cement weight basis).

Figure 18 plots bar weight loss on an annual percentage basis versus admixed Cl⁻ concentration for specimens with bars at both depths. This indicates that weight loss was highest for carbon steel and lowest for the Type 316 stainless steels. The other austenitics performed comparably. In general, corrosion rate increased with increasing Cl⁻, the effect being greatest for the carbon steel and minimal for the austenitics. In addition, corrosion intensity was greater for the lower cover steel and increased in proportion to the admixed Cl⁻ concentration above 0.96 w/o. No explanation is apparent as to why the carbon steel exhibited higher corrosion rate with 0 compared to 0.32 and

0.96 w/o admixed Cl⁻. The ferritics performed satisfactorily at the lower Cl⁻
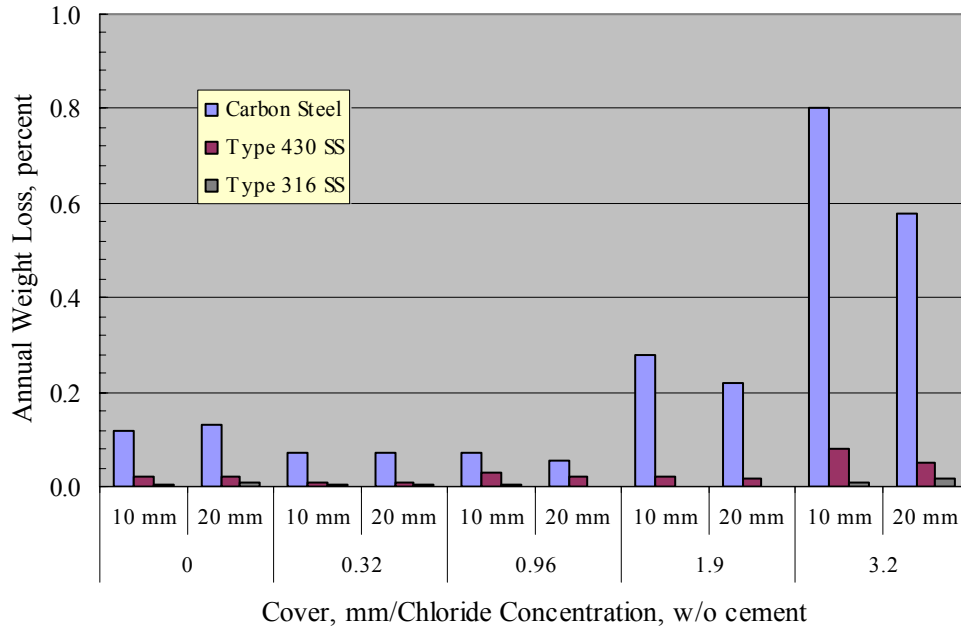concentrations, but suffered severe pitting at the higher concentrations.

Figure 18. Weight loss of different reinforcements during a 10-year United Kingdom
  exposure.

Corrosion resistance of a ferritic stainless steels was also investigated by Callaghan
and Hearn who exposed 12 w/o Cr reinforcement with 12 and 25 mm cover in relatively
poor quality concrete prisms (no admixed Cl⁻) to a severe marine environment for 4.5
years.[42] Severe pitting occurred on reinforcement in companion black bar specimens,
whereas attack on the stainless steels was minimal. The authors reasoned that the good
performance of the ferritic stainless steels in their exposures, compared to that of
Treadaway et al., resulted from chlorides not being admixed such that a more protective
passive film formed.[41] It was concluded that such stainless steels may be the best choice
for moderately aggressive environments.

McDonald et al. performed a series of exposures using double matted concrete slab
specimens with a range of reinforcement types that included Types 304 and 316 stainless
steels.[43] The average cement content and w/c were 370 kg/m³ and 0.47, respectively,
and clear cover was 25 mm. The exposures involved 4 days wetting with 15 w/o NaCl at
16–27 °C and 3 days drying at 38 °C for 12 weeks, followed by 12 weeks of continuous
ponding. The cycle then was repeated.

Average macrocell current density (anodic) on straight black bar control specimens
during the 96-week tests, which was determined as the voltage drop across a 10 Ω

resistor between the top and bottom bars, was 27.6 mA/m^2, or 0.03 mm/year.[1] All specimens were cracked after 48 weeks. For specimens with straight and bent Type 304 SS reinforcement in both mats and with both cracked and uncracked concrete, macrocell current density was 0.016–0.039 mA/m^2, or 0.0002–0.0005 mm/year. However, for sound slabs with black bottom bars, this current density was 8.8 mA/m^2 (0.01 mm/year), and minor rust staining was apparent on the concrete surface. For cracked slabs with black bottom bars, current density was even higher at 20.8 mA/m^2 (0.02 mm/year). No surface staining was noted on this last specimen type, nor for any Type 304 stainless steel reinforcements.

That Type 304 SS top reinforcement exhibited corrosion when coupled to black bottom bars is surprising, because it requires potential of the black bars minus voltage drop between the two mats to be more positive than ϕ_{crit} of the stainless steel. This finding contrasts with the results of Hope, who performed dual compartment aqueous exposures of stainless steel-black steel couples and concluded that these two reinforcement types could be mixed, provided concrete surrounding the black bars remained Cl$^-$-free.[44] Even if chlorides are present here, the black bars should corrode and provide galvanic cathodic protection to the stainless steel.

In contrast, macrocell corrosion rate for slabs with Type 316 stainless steel reinforcement was in the range 0.039–0.070 mA/m^2 (0.0005–0.0009 mm/year), irrespective of the presence of a concrete crack or a black bar bottom mat. No rust staining or concrete cracking was noted.

Clemeña and Virmani reported results for 0.5 w/c concrete slabs that were exposed outdoors in Virginia to successive 3 days wet–4 days dry cycles using a saturated NaCl solution for 700 days.[45] Reinforcement types, which were both bent and straight, included carbon steel, Types 304, 316LN, and 2205 stainless steels, and Type 316 stainless steel clad bars. Clear cover over the reinforcement was 25 mm. Some of the clad bars contained two intentionally drilled 3 mm diameter holes that extended to the carbon steel core. Slabs for which the top bars were stainless steel and bottom bars were carbon steel were included. Researchers came to the following conclusions:

1. In all cases, potential became progressively more negative as exposure time increased, and after 700 days was approximately -550 mV$_{CSE}$ (-480 mV$_{SCE}$) for the carbon steel and -300 mV$_{CSE}$ (-230 mV$_{SCE}$) for the stainless steels. The carbon steel slabs exhibited corrosion and concrete cracking, whereas no damage was apparent for the stainless steel slabs.

2. The mean macrocell current density for slabs with carbon steel top bars averaged 6.36 mA/m^2 (0.007 mm/year), whereas for the stainless steel specimens, this current was either zero or negative. Polarization resistance determinations showed corrosion rates to average 24.1 mA/m^2 (0.03 mm/year) for the carbon

---

[1] This review employs the units used by the original authors. The following conversions may be used for converting between the different units:

 1 mA/m^2 = 0.1 μA/cm^2 = 0.011 mm/year = 11.5 μm/year = 0.43 mils/year.

steel and 0.8 mA/m^2 (0.0009 mm/year) for the stainless steel, with relatively little difference between alloys in the carbon steel category. In addition, the general trend was that the carbon steel's corrosion rate increased with time, but this parameter was relatively constant for the stainless steels.

3. Corrosion rate for the stainless clad reinforcement was essentially the same as that for the solid stainless bars. Also, no detrimental consequence of exposed core material at the intentional cladding defects, as indicated by potential, macrocell current, or polarization resistance, was apparent.

Rasheeduzzafar et al. also conducted outdoor exposures in eastern Saudi Arabia of concrete specimens reinforced with black, galvanized, ECR, and stainless clad reinforcing bars.[46] The mix design consisted of 390 kg/m^3 Type V cement, w/c = 0.45, and admixed Cl$^-$ concentrations as NaCl of 2.4, 4.8, and 19.2 kg/m^3. Clear cover was 25 mm. No details regarding the clad alloy were provided. After 7 years, the clad-reinforced slabs exhibited no indications of corrosion or cracking, whereas cracks were present in at least some of the slabs with each of the other reinforcement types.

Flint and Cox performed a series of seawater immersion and tidal exposures on concrete specimens with partly embedded Type 316 SS for up to 12.5 years.[47] This study focused on the possibility of crevice corrosion at the steel-concrete interface. Such attack was negligible but with some corrosion occurring at the steel-concrete-seawater interface, as has been reported to be particularly significant in the case of carbon steel reinforcement.[48]

Cross-Procedural Experiments

Several authors have conducted experimental programs that involved various combinations of aqueous solution, mortar-coated, and concrete embedded exposures. Among these are the tests of Darwin et al., who employed a two-compartment galvanic cell with simulated pore solution and mortar chunks in both compartments and 1.6 molal NaCl in one and no Cl$^-$ in the other.[49] In one set of tests, bare or uncoated specimens were employed; in a second set of tests, the specimens were mortar coated. In a third set, both sound and cracked macrocell-type concrete slab specimens were subjected to the Southern Exposure protocol.[50] Results were reported in terms of corrosion rate as determined from macrocell current, rather than c_{th}, with the stated reason being that the latter parameter is achieved quickly in the vicinity of concrete cracks, such that all reinforcement types are likely to corrode at these locations. This rationale may be appropriate for some, but not all, types of reinforcement.

Figure 19 shows typical results for mortar-coated, aqueous solution exposed specimens during the 15-week period. Generally, corrosion rates were approximately constant after about week 10. On this basis, the long-term corrosion rate of black steel was highest. The rate for MMFX™ was approximately a factor of 2 less, while that for 2201 (unpickled) was less an additional factor of 2. In contrast, corrosion rates for 2201P (pickled), 2205, and 2205P (pickled) were typically 0.1 μm/year (0.086 mA/m^2) or less.

Also, although there was no significant distinction between the corrosion rates for 2205 and 2205P, the rate for 2201 exceeded that for 2201P.
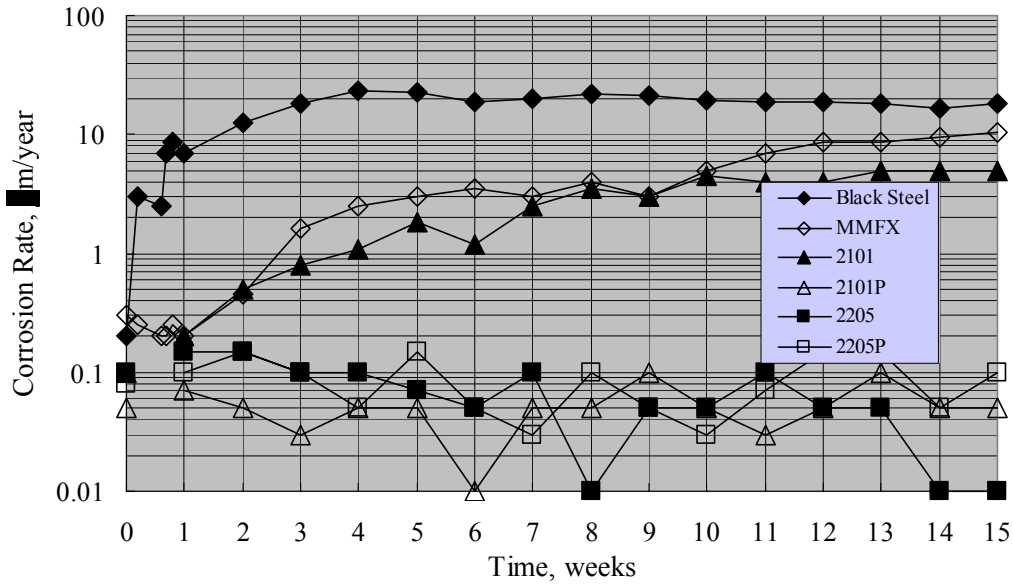
Figure 19. Corrosion rate of various mortar-coated reinforcement types in an aqueous macrocell test arrangement.

Figure 20 shows the average corrosion rate for the different reinforcement types during 48 weeks of Southern Exposure. These data are qualitatively consistent with those from the mortar-coated tests, although steady state appears to have been reached for the more active metals in the case of Southern Exposure; but it is unclear that this was always so for the mortar coated specimens. Corrosion rate for the stainless steels was consistently 2–3 orders of magnitude less than for the actively corroding reinforcements. Also, alloys that performed well apparently remained passive, irrespective of test condition.

37

Figure 20. Corrosion rate of various reinforcement types in concrete slabs
undergoing Southern Exposure testing.

As noted above, there was a difference in performance for 2201 SS but not 2205 SS
in the aqueous exposures, depending on surface treatment (as-received versus pickled).
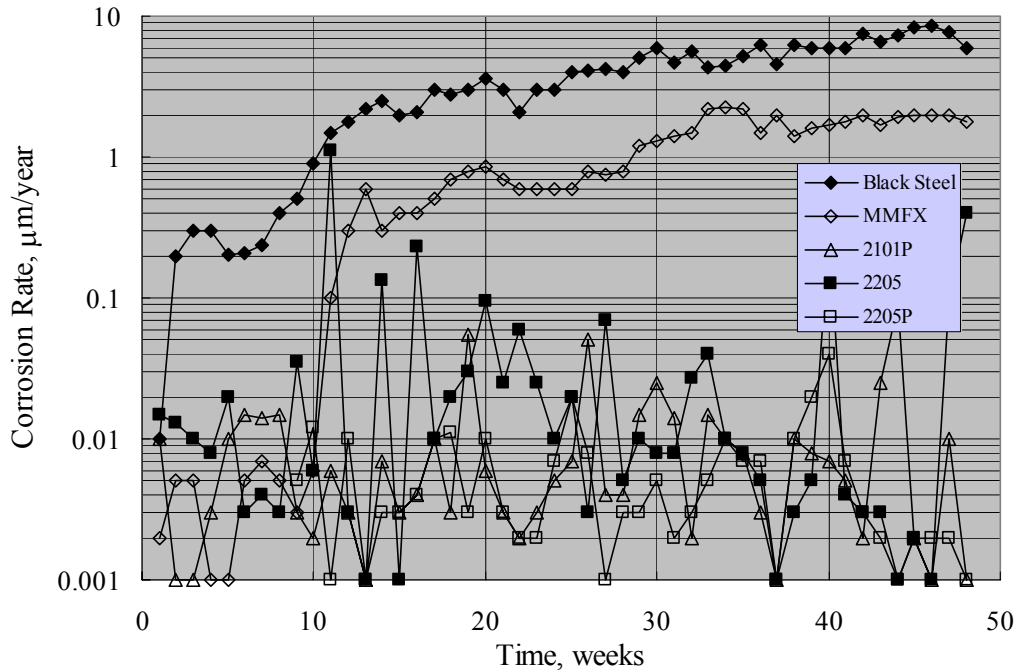Unpickled specimens were not included in the Southern Exposure concrete specimens, so
no such comparison is possible here. This distinction between specimens with the two
preparation methods apparently resulted because surface penetrating nonmetallic
inclusions or iron/steel particles from handling equipment became embedded and
corroded (or both). This leaves surface irregularities that, for metals with relatively low
passivation tendency in a sufficiently high Cl⁻ concentration electrolyte, can result in pit
initiation according to the mechanism described above.

Figure 21 compares corrosion rates for the different environments investigated by
Darwin et al. and indicates that these increased generally in proportion to the anticipated
conductivity of the electrolyte (highest corrosion rates in the aqueous solution and lowest
in sound concrete).[53] Comparisons here should be made with caution, however, because
bars with little or no tendency for passivation (black steel) were apparently active upon
initial exposure, whereas bars with an intermediate passivation tendency apparently either
activated slowly, or active corrosion spread progressively with time. On this basis, the
low resistivity electrolyte test conditions with high initial Cl⁻ failed to provide due credit
for a corrosion initiation period, which may be extensive. As such, the aqueous
exposures provide information on which different reinforcements can be ranked, but do
not facilitate life-prediction modeling. This rationale disregards the presence of mortar or
concrete cracks, however. If (1) chlorides accumulate rapidly at the base of these cracks,
(2) the resulting corrosion initiates early in the structure's life cycle, and (3) this
corrosion controls service life, then the data can be viewed as applicable.
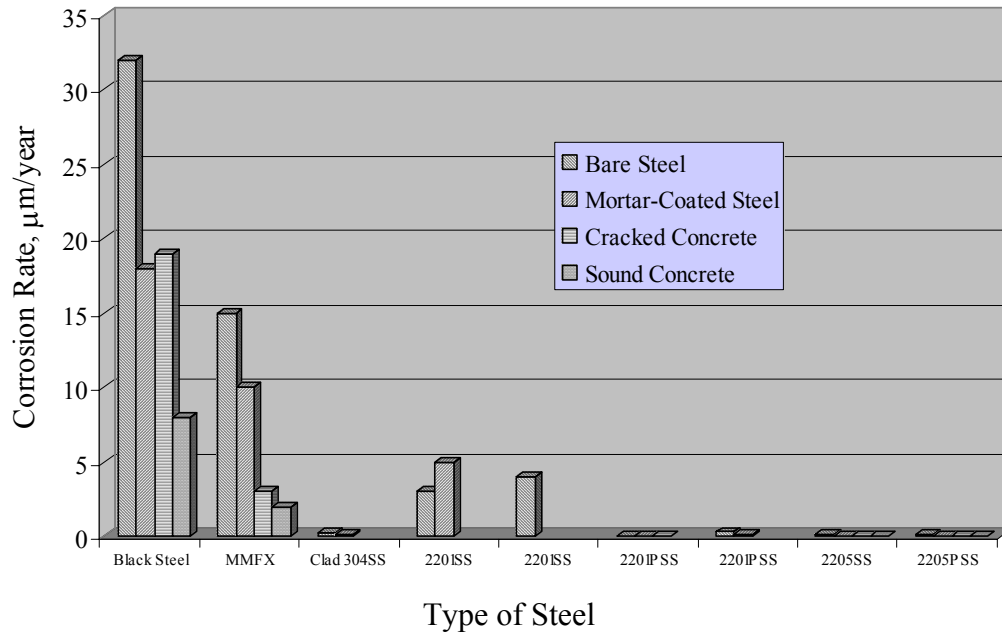
Figure 21. Comparison of corrosion rates in the different environments (multiple listings of same alloy represent results for duplicate specimens).

Specific Reinforcement Alloys

General

Data for several relatively unique corrosion-resistant alloys (in addition to the standard ferritic, austenitic, and duplex SSs) were represented in some of the assessments discussed above. These include Nitronic 33, MMFX, 3Cr12™, and clad SS. Each of these is discussed in greater detail below.

Nitronic 33

Limited data for Nitronic 33, which conforms to American Society for Testing and Materials (ASTM) Specification A580, Grade XM-29, were reported above in conjunction with tables 3 and 4 and figure 8. In addition, Jenkins reported the results of laboratory aqueous exposures and field evaluations.[51] This alloy is of particular interest to the U.S. Navy because of its nonmagnetic properties in addition to relatively good corrosion resistance and high strength. Nominally, the composition of Nitronic 33 is 18 percent Cr, 12 percent Mn, and 3.5 percent Ni. The material tested by Jenkins had a yield strength of 800 MPa. Potentiodynamic polarization scans in aqueous solutions indicated a full range of passivity for pH = 12.1, 11.6, and 11.2 and Cl⁻ concentrations of 0–6,000 parts per million (ppm). At pH 10.0, full passivity was exhibited at a Cl⁻ concentration of 2,000 ppm, but at 6,000 ppm, ϕ_{crit} was +100 mV (reference electrode not stated). The

program also involved evaluating driven piles that were placed at the Port of Tacoma, WA. No Nitronic 33 corrosion activity was detected, although age of the pilings was only 17 months when measurements were taken.

MMFX

Within the past several years, a proprietary alloy, initially designated as MMFX (subsequently MMFX-I and then MMFX-II), has been marketed as a CRR alternative for concrete bridge deck service. Composition is nominally that of low carbon steel but with 9–10 w/o Cr. As such, it does not meet the classification of stainless steel, because a minimum of 12 w/o Cr is required for this designation. Nonetheless, such a Cr amount may contribute to enhanced corrosion resistance compared to carbon steel. Mechanical strength of MMFX exceeds that of conventional reinforcement. For example, Darwin et al. determined the average 0.2 percent offset yield strength, tensile strength, and elongation for 5 specimens in each of 3 heats as 910 MPa, 1139 MPa, and 7.1 percent, respectively.[52]

Corrosion resistance of this steel is ascribed to a special thermomechanical treatment that yields a microstructure comprised of packet martensite and nanosheets of untransformed austenite. This is stated to reduce or eliminate microcells that otherwise cause corrosion. However, microcells invariably exist irrespective of microstructure. Also, it is unclear why microcells should necessarily be a factor in bridge deck service where corrosion, once initiated, is controlled predominantly by macrocells. It can be reasoned that the MMFX microstructure may have a reduced exchange current density for the oxygen or hydrogen reduction reactions (or for both), in which case reduced corrosion rate could result. Corrosion data for MMFX, as reported by Darwin et al., were indicated above in conjunction with figures 20 and 21, where a reduced rate compared to carbon steel by a factor of 2–3 is apparent.[53] In addition, Lopez conducted salt fog exposures of MMFX specimens to 1,000 hours using 5 w/o NaCl and a repetitive 1-hour fog (ambient temperature)–1-hour dry (35 $^{\circ}$C) cycle; the results are shown in figure 22.[53] While the data scatter is relatively large, corrosion rate of the MMFX was, on average, 44 percent less than for the carbon steel. It should be interesting to determine via parallel experiments if corrosion performance of MMFX in concrete service affords any advantage compared to 12 w/o Cr ferritic SSs (see below).
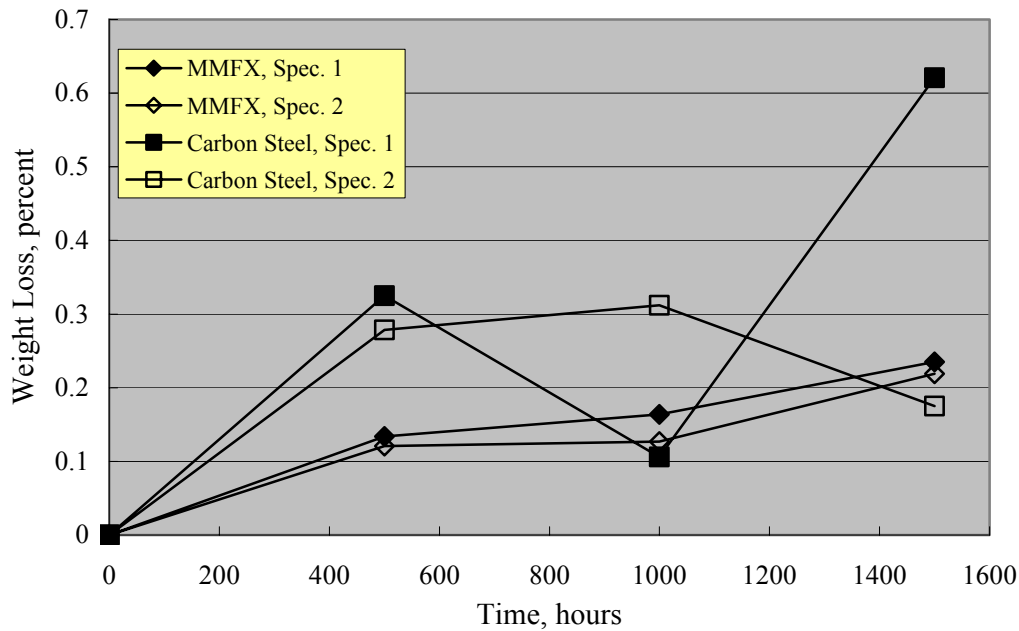
Figure 22. Corrosion rate of MMFX and carbon steel under cyclic salt fog exposure.

Also of concern is the relatively high strength of MMFX compared to carbon steel reinforcement. Based on concrete beam tests, Ansley concluded that designers using MMFX reinforcement should consider detailing and the lack of a distinct yield point for this material.[54] Ansley also indicated that lap splices and hook elements that are adequate for Grade 60 reinforcement may be insufficient with MMFX.

Proprietary Ferritic Stainless Steels

Ferritic stainless steels, designated as 3Cr12 and CRS 100, with approximately 12 w/o Cr are being produced as reinforcement. The composition of these is essentially the same; the 3Cr12 conforms to European Standard EN 10088 Grade 1.4003. These are relatively low-cost alternatives to Types 304 and 316 and may prove suitable choices for moderate, although probably not severe, chloride exposures.

Clad Stainless Steel

Bars of this type are potentially available from two suppliers. Both employ Type 316 stainless steel as the cladding and innovative manufacturing technologies. One company packs a stainless tube with carbon steel scrap and hot rolls this into reinforcing bars. This production method allows any cladding alloy to be employed instead of 316 SS, with cost varying accordingly. The other company plasma-coats steel billets and then rolls these. The plasma method lacks the flexibility of the first method, because the technology is relatively insensitive to clad material cost.

Several of the evaluation programs noted above included clad SS reinforcement.[39,48] As such, clad bars potentially afford the corrosion resistance of the

SS cladding but at a reduced cost compared to solid SS bars. Concerns include corrosion at cut ends where the carbon steel core is exposed and corrosion at cladding defects. On one hand, the relatively small anode-to-cathode area ratio that is likely to accompany clad defects or exposed bar ends should facilitate such an attack. On the other hand, stainless steels serve as a relatively poor catalytic surface for the cathode reaction, as revealed by the experiments of Sorensen et al., who performed potentiodynamic polarization scans and determined that the current density at -700 mV_{SCE} was 9 ±2 mA/m^2 for Type 304 SS, 31 ±11 mA/m^2 for Type 316, and 143 ±68 mA/m^2 for carbon steel.[42]

Cui and Sagüés[55,56] and Clemeña and Virmani[49] both exposed concrete specimens containing SS clad reinforcement, where holes had been drilled intentionally through the cladding to the carbon steel core. In the Cui and Sagüés experiments, the concrete was admixed with either 5 or 8 w/o Cl^- (cement weight basis) and exposed indoors under ambient laboratory conditions or at 40 ^{o}C and 100 percent relative humidity. Clemeña's and Virmani's experiments were wet-dry cyclic ponded with a saturated NaCl solution, as noted above. Cui and Sagüés measured corrosion activity at the clad defect sites, although the magnitude of this tended to moderate with time in some cases. This finding that corrosion moderated with time was attributed to progressively developing corrosion products.

Companion numerical modeling results were in general agreement with the experimental findings, and predicted that corrosion rate should increase with increasing defect size and decrease with increasing concrete resistivity. For a 1 mm diameter clad break and 30 kΩ·cm concrete, corrosion rate was projected as approximately 14 mA/m^2 (0.18 mm/year). Clemeña and Virmani, however, reported no electrochemical indications of corrosion on their clad bars with defects after 700 days' exposure.[49] This could have resulted because their specimens contained no admixed chlorides, such that time was provided before chlorides arrived at the steel depth for the passive film to stabilize. Clearly, more experimental information is needed before definitive conclusions can be reached regarding the importance of exposed carbon steel core material.

Actual Structures

While there has been only limited utilization of CRR in concrete construction to date, a small inventory of such structures does exist, nonetheless. These can provide information that can be used to develop a database of experience. A summary of these structures is provided below.

Progresso Pier

Probably the best example of stainless steel reinforced concrete structures in aggressive, Cl^- environments is the 1,752-m long pier at the Port of Progreso de Castro in Yucatán, Mexico. Constructed between 1939–1941, the pier is now more than 60 years old. Approximately 200,000 kg of 30 mm diameter, nondeformed Type 304 SS was employed. The pier consists of 146 12-m span hinged arches, each of which is supported

at the ends by reinforced girders positioned on massive nonreinforced concrete piles. Figure 23 shows a general photograph of the pier.

Several inspections and evaluations of the pier condition have been performed during the past decade.[57,58] These have indicated no visible signs of deterioration, despite the fact that no maintenance apparently has been performed. Figure 24 shows a photograph of two arches and piling and reveals the generally good condition of the structure. It has been determined that the concrete is of relatively poor quality with a w/c of 0.50–0.70, porosity 19–24 percent, and resistivity 0.6–2.5 kΩ·cm. Based on acid soluble analyses of samples from two cores, Cl$^-$ concentration at the bar depth (78 mm) was determined as 1.2 w/o concrete. This, coupled with the tropical marine environment, constitutes severe exposure conditions for the reinforcement. In the most recent inspection, no corrosion stains or corrosion-induced cracks were observed along the entire structure.[61] However, stress corrosion cracking (SCC) was stated to have affected exposed bent end hooks. Occurrence of SCC in Type 304 SS in near-neutral or alkaline Cl$^-$ environments at ambient temperatures is unexpected and warrants further investigation. Also, severe localized corrosion was noted at a location where the reinforcement had been exposed previously. Figure 25 provides a photograph of this damage.

(photograph courtesy of Dr. E.I. Moreno)

Figure 23. Perspective view of the Progresso pier.

Detroit, MI (Interstate (I)-696 over Lenox Road)

As a part of this bridge construction project, Type 304 SS reinforcement was placed in the eastbound lanes in 1984, and ECR was used in the westbound lanes. During an inspection in 1993, cores were removed from the eastbound lanes to assess the concrete and reinforcement. Three of the cores contained 16 mm diameter reinforcement. No concrete cracking that could be attributed to corrosion was noted, neither on the bridge generally nor in the cores. Minor corrosion staining in conjunction with a noncorrosion-related crack was apparent on one of the extracted bar sections. Acid soluble Cl⁻ determinations at the reinforcement depth (75–165 mm) indicated values of 0.54, 0.26,

Figure 24. Photograph of hinged arches and piling.

Figure 25. Corrosion of an exposed reinforcing bar.

and 0.22 w/o cement (0.078, 0.037, and 0.032 w/o concrete) for the three cores, which is near the threshold for black steel. The inspection and analysis results are described in greater detail elsewhere.[59]

Trenton, NJ (I-295 over Arena Drive)

The northbound and southbound bridges for this project were constructed in 1983–1984 using ECR in the northbound bridge and Type 304 clad SS from a source in England in the southbound bridge. The design employed steel girders, stay-in-place metal decking, a reinforced concrete bridge deck, and a 25–37 mm latex-modified concrete overlay. During an inspection in 1993, minor delamination of the overlay was detected in some locations.[59] Four cores, two from delaminated and two from sound locations, containing a total of nine clad SS segments, were acquired. No corrosion was apparent on any of these, except beneath a plastic capped cut bar end where the carbon steel core was exposed. This attack was attributed to a low pH environment that

44

developed here, such that passivity was not maintained. No adhesive had been used in conjunction with placing the cap. Acid soluble Cl⁻ concentration at the steel depth (50–62 mm including overlay) was low and in the range 0.009–0.013 w/o concrete.

Ontario, Canada

In 1996, a 21-m long, single-span bridge was constructed as a demonstration project on Highway 407 over Mullet Creek in Ontario, Canada. The two-lane structure consists of a 235-mm thick concrete deck slab reinforced with 11,000 kg of Type 316LN SS in both mats at a design cover for the upper mat of 80 ±20 mm on prestressed concrete I-beams. Probes were installed for corrosion monitoring purposes. The SS was shipped in coils that subsequently were straightened using conventional carbon steel equipment. This resulted in iron embeddments that were visually unappealing but did not compromise performance. Inspections performed within the first year of construction revealed corrosion potentials for the reinforcement in the passive range (-0.26 V_{CSE} with standard deviation 0.06). Minor shrinkage cracks were disclosed on parapet walls but with none on the deck.[60]

In 1998, the Ontario Ministry of Transportation (OMT) established a policy that the top mat of 400 series bridges (100,000 or more vehicles per day) and all barrier walls would be stainless steel. Requiring this for the top mat only was based on a research study that showed no occurrence of corrosion for black steel electrically connected to Types 316LN or 2205 stainless steels, as long as chlorides were not present at the black steel.[61]

In conjunction with the above policy, OMT constructed a two-lane, three-span, continuous 225-mm thick by 37.5-m long concrete deck on galvanized steel plate girders bridge on Highway 9 over the South Holland Canal in Ontario, Canada, in 1999 using Type 316L stainless steel clad bars as the top mat. Despite bar quality control and delivery schedule issues, researchers concluded that the use of this reinforcement type is viable.[62]

DISCUSSION

The literature that was reviewed clearly indicates that the high-performance reinforcement types identified outperform black bar from a corrosion-resistance perspective in bridge structure service. A complicating aspect of high-performance reinforcement, unlike the case of black bar, is that numerous types with a broad range properties are available. Because enhanced corrosion performance depends primarily on the concentration of relatively costly alloying elements such as Cr and Mo and to a lesser extent upon surface treatment, the better performers are the most expensive. The most logical approach is to select the alternative that will perform satisfactorily for the design life at the lowest life cycle cost. However, accomplishing this requires knowing the long-term performance of candidate reinforcement types; in other words, being able to anticipate the design life of the bridge in question, which can be 75–100 years. Presently, such information can only be obtained from accelerated, short-term tests, but there is no reliable correlation between these results and long-term performance.

BIBLIOGRAPHY

1. Virmani, Y.P, Jones, W.R., and Jones, D.H., *Public Roads,* Vol. 84(3), 1984, p. 96.

2. Koch, G.H., Brongers, P.H., Thompson, N.G., Virmani, Y.P, and Payer, J.H., *Corrosion Costs and Prevention Strategies in the United States*, Report No. FHWA-RD-01-156, Federal Highway Administration, Washington, DC, March 2002.

3. Yunovich, M, Thompson, N.G., and Virmani, Y.P., "Life Cycle Cost Analysis for Reinforced Concrete Bridge Decks," Paper No. 03309 presented at CORROSION/03, San Diego, CA, March 10-14, 2003.

4. Hausmann, D.A., *Materials Protection*, Vol. 6(10), 1967, p. 19.

5. Li, L. and Sagüés, A.A., *Corrosion*, Vol. 57, 2001, p. 19.

6. Sandberg, P. and Larsson, J., "Chloride Binding in Cement Pastes in Equilibrium with Synthetic Pore Solutions," in *Chloride Penetration in Concrete Structures*," Nordic Miniseminar, Göteborg, January 1993, Ed. L.-O. Nilsson (Chalmers Tekniska Hogskola, Göteborg), 1993, p. 98.

7. Tritthart, J., *Cement and Concrete Research*, Vol. 19, 1989, p. 683.

8. Glass, G.K. and Buenfeld, N.R., "Chloride Threshold Levels for Corrosion-induced Deterioration of Steel in Concrete," Paper No. 3 presented at RILEM International Workshop on Chloride Penetration into Concrete, Saint Rémy-les-Chevreuse, France, October 15-18, 1995.

9. Bentur, A., Diamond, S, and Berke, N.S., *Steel Corrosion in Concrete*, E&FN Spon, London, UK, 1997, pp. 15-16.

10. Code of Federal Regulations, Section 650.305, "Frequency of Inspections," U.S. Government Printing Office, Washington, DC, April 1, 2002 revision.

11. Tutti, K., *Corrosion of Steel in Concrete*, Report No. 4, Swedish Cement and Concrete Research Institute, Stockholm, Sweden, 1982.

12. Virmani, Y.P. and Clemena, G.G., *Corrosion Protection: Concrete Bridges*, Report No. FHWA-RD-98-088, Federal Highway Administration, Washington, DC, September 1998.

13. Powers, R.G. and Kessler, R., *Corrosion Evaluation of Substructure, Long Key Bridge*, Corrosion Report No. 87-9A, Florida Department of Transportation, Gainesville, FL, 1987.

14. Powers, R.G., *Corrosion of Epoxy-Coated Rebar, Keys Segmental Bridges Monroe County*, Report No. 88-8A, Florida Department of Transportation, Gainesville, FL, August, 1988.

15. Zayed, A.M. and Sagues, A.A., "Corrosion of Epoxy-Coated Reinforcing Steel in Concrete," Paper No. 386 presented at CORROSION/89, New Orleans, LA, April 21, 1989.

16. Gustafson, D.P., "Epoxy Update," *Civil Engineering*, Vol. 58, No. 10, 1988, pp. 38-41.

17. Houston, J.T., Atimay, E., and Ferguson, P.M., *Corrosion of Reinforcing Steel Embedded in Structural Concrete*, Report No. CFHR-3-5-68-112-1F, Center for Highway Research, University of Texas, Austin, TX, 1972.

18. Ryell, J. and Richardson, B.S., *Cracks in Concrete Bridge Decks and Their Contribution to Corrosion of Reinforcing Steel and Prestressed Cables*, Report No. IR51, Ontario Ministry of Transportation and Commission, Ontario, Canada, 1972.

19. Bamforth, P.B., "Definition of Exposure Classes and Concrete Mix Requirements for Chloride Contaminated Environments," *Corrosion of Reinforcement in Concrete*, Eds: Page, C.L., Treadaway, K.W.J., and Bamforth, P.B., Society of Chemical Industry, London, UK, 1996, p. 176.

20. Howell, K.M. and Tinnea, J.S., "Corrosion Investigation and Mitigation of Reinforcing Steel Viaducts," Paper No. 00797 presented at CORROSION/00, Orlando, FL, March 26-31, 2000.

21. Bamforth, P.B. and Price, W.F., "Factors Influencing Chloride Ingress into Marine Structures," *Concrete 2000*, Eds: Dhir, R.K. and Jones, M.R., E&FN Spon, London, UK, 1993, p. 1105.

22. Standard Recommended Practice RP0290-2000, "Impressed Current Cathodic Protection of Reinforcing Steel in Atmospherically Exposed Concrete Structures," NACE International, Houston, TX, 2000.

23. Miller, J.B., "Structural Aspects of High Powered Electrochemical Treatment of Reinforced Concrete," in *Corrosion and Corrosion Protection of Steel in Concrete*," Ed. R.N. Swamy, Elsevier Applied Science, London, UK, 1994, p. 29.

24. State-of-the-Art Report 01101, "Electrochemical Chloride Extraction from Steel Reinforced Concrete," NACE International, Houston, TX, 2001.

25. Andrade, C. and Macias, A., "Galvanized Reinforcement in Concrete," in *Surface Coatings-2*, Ed. A.D. Wilson, .W. Nicholson, and H.J. Posser, Elsevier Applied Science, London, UK, p. 137.

26. Andrade, C., Holst, J.D., Nurenberger, U., Whiteley, J.D., and Woodman, N., *Protection Systems for Reinforcement*, CEB Information Bulletin No. 211, Switzerland, 1992.

27. Bower, J.E., Friedersdorf, L.E., Heuhart, B.H., Marder, A.R., and Juda, A.I., *Application of Stainless Steel and Stainless-Clad Reinforcing Bars in Highway Construction*, Report No. HWA-PA-2000-011+96-31(04), Pennsylvania Department of Transportation, University Park, PA, November 27, 2000.

28. Wheat, H.G. and Deshpande, P.G., "Alternative Reinforcement Materials for Concrete—A State of the Art Review," Paper No. 01652 presented at CORROSION/01, Houston, TX, March 11-16, 2001.

29. McDonald, J.B., Pfiefer, D.F., and Blake, G.T., *The Corrosion Performance of Inorganic-, Ceramic-, and Metallic-Clad Reinforcing Bars and Solid Metallic Reinforcing Bars in Accelerated Screening Tests*, Report No. FHWA-RD-96-085, Federal Highway Administration, Washington, DC, October 1996.

30. *Stainless Steel in Concrete—State of the Art Report*, European Federation of Corrosion Publication No. 18, Ed. U. Nürnberger, Institute of Materials, Cambridge University Press, Cambridge, UK, 1996.

31. A615/A615M "Specification for Deformed and Plain Billet-Steel Bars for Concrete Reinforcement," *Annual Book of Standards*, American Society for Testing and Materials, Philadelphia, PA, 2004.

32. Wilde, B.E., "A Critical Appraisal of Some Popular Laboratory Electrochemical Tests for Prediction the Localized Corrosion Resistance of Stainless Steel in Sea Water," *Corrosion*, Vol. 28, 1972, p. 283.

33. Galvele, J.R., "Transport Processes and the Mechanism of Pitting of Metals," *Journal of the Electrochemical Society*, Vol. 123, April 1976, p.464-474.

34. Galvele, J.R., "Transport Processes in Passivation Breakdown—II. Full Hydrolysis of the Metal Ions," *Corrosion Science*, Vol. 21(8), 1981, p.551-579.

35. Muller, I.L. and J.R. Gavele, "Pitting Potential of High Purity Aluminum Alloys—II. Al-Mg and Al-Zn Alloys," *Corrosion Science*, Vol. 17, 1977, p. 995-1007.

36. Hurley, M.F. and Scully, J.R., "Chloride Threshold Levels in Clad 316L and Solid 316LN Stainless Steel Rebar," Paper No. 02224 presented at CORROSION/02, Denver, CO, 2002.

37. Bertonini, L., Bolzoni, T., Pastore, P., and Pedeferri, P., "Behavior of Stainless Steel in Simulated Concrete pore Solution," *British Corrosion Journal*, Vol. 31, 1996, p. 218.

38. Sorensen, B., Jensen, P.B., and Maahn, E., "The Corrosion Properties of Stainless Steel Reinforcement," in *Corrosion of Reinforcement in Concrete*, Ed. C.L. Page et al., Elsevier, London, UK, 1990, pp. 601-605.

39. Nurnberger, U., Beul, W., and Onuseit, G., "Corrosion Behavior of Welded Stainless Reinforced Steel in Concrete," *Otto-Graf-Journal*, Vol. 4, 1993, p. 225.

40. Treadaway, K.W.J., "Corrosion of Steel Reinforcement in Concrete Construction," *Materials Preservation Group*, Society of Chemical Industry, London, UK, 1978.

41. Treadaway, K.W.J., Cox, R.N., and Brown, B.L., "Proceedings," *Institution of Civil Engineers*, Part 1, Vol. 86, 1989, p. 305.

42. Callaghan, B.G. and Hearn, I.R., "The Use of 3Cr12 as Reinforcing in Concrete," paper presented to the South African Corrosion Institute, Cape Town, South Africa, April 1989.

43. McDonald, J.B., Pfiefer, D.F., and Sherman, M.R., *Corrosion Evaluation of Epoxy-Coated, Metallic-Clad, and Solid Metallic Reinforcing Bars in Concrete*, Report No. FHWA-RD-98-153, Federal Highway Administration, Washington, DC, December 1998.

44. Hope, B.B., *Some Corrosion Aspects of Stainless Steel Reinforcement in Concrete Bridges*, Report No. MI-181, Ontario Ministry of Transportation, November 24, 2000.

45. Clemeña, G.G and Virmani, Y.P., "Comparison of the Corrosion Resistance of Selected Metallic Reinforcing Bars for Extension of Service Life of Future Concrete Bridges in Outdoor Concrete Blocks," Paper No. 03298 presented at CORROSION/03, San Diego, CA, March 16-20, 2003.

46. Rasheeduzzafar, Dakhil, F.H., Bader, M.A., and Khan, M.M., "Performance of Corrosion Resisting Steels in Chloride-Bearing Concrete," *ACI Materials Journal*, September-October, 1992, p. 439.

47. Flint, G.N. and Cox, R.N., "The Resistance of Stainless Steel Partly Embedded in Concrete to Corrosion by Seawater," *Magazine of Concrete Research*, Vol. 40, 1988, p. 13.

48. Miller, R.L., Hartt, W.H., and Brown, R.P., "Stary Current and Galvanic Corrosion of Reinforcing Steel in Concrete," *Materials Performance*, Vol. 15(5), 1976, p. 20.

49. Darwin, D., Browning, J., Balma, J., Ji, J., Gong, L., Nguyen, T.V., and Locke, C.E., "Corrosion Resistant Reinforcing Steel," paper presented at the Concrete Bridge Conference, Chicago, IL, Oct. 9, 2002,.

50. Pfeifer, D.W. and Scali, M.J., "Concrete Sealers for Protection of Bridge Substructures," *National Cooperative Highway Research Program Report 244*, Transportation Research Board, National Research Council, Washington, DC, December 1981.

51. Jenkins, J.F., *Validation of Nitronic 33 in Reinforced and Prestressed Concrete*, Report No. TN-1764, Naval Civil Engineering Laboratory, Port Hueneme, CA, July 1986.

52. Darwin, D., Browning, J., Nguyen, T.V., and Locke, C.E., *Mechanical and Corrosion Properties of a High Strength, High Chromium Reinforcing Steel for Concrete*, Report No. SD2001-05-F, South Dakota Department of Transportation, Pierre, SD, March 2002.

53. Lopez, J., New Jersey Department of Transportation, unpublished research.

54. Ansley, M.H., *Investigation into the Structural Performance of MMFX Reinforcing*, Florida Department of Transportation Structures Laboratory, Tallahassee, FL, September 2002.

55. Cui, F. and Sagüés, A.A., "Corrosion Behavior of Stainless Clad Rebar," Paper No. 01645 presented at CORROSION/01, Houston, TX, March 11-16, 2001.

56. Cui, F. and Sagüés, A.A., "Corrosion Performance of Stainless Steel Clad Reinforcing Bar in Concrete," Paper No. 03310 presented at CORROSION/03, San Diego, CA, March 16-20, 2003.

57. "Pier in Progreso, Mexico: Inspection Report Evaluation of the Stainless Steel Reinforcement," RAMBØLL Consulting Engineers and Planners, Denmark, March 1999.

58. Castro-Borges, P., de Rincón, O.T, Moreno, E.I., Torres-Acosta, A.A., Martínez-Madrid, M., and Knudsen, A., "Performance of a 60-Year-Old Concrete Pier with Stainless Steel Reinforcement," *Materials Performance*, Vol. 41(10), 2002, p. 50.

59. McDonald, D.B., Sherman, M.R., Pfeifer, D.W., and Virmani, Y.P., "Stainless Steel Reinforcing as Corrosion Protection," *Concrete International*, May 1995.

60. Ip, A.K.C, Pianca, F., and Hope, B.B, "Application of Stainless Steel Reinforcement for Highway Bridges in Ontario," paper presented at the CONSEA Conference, Norway, 1998.

61. Hope, B.B., *Some Corrosion Aspects of Stainless Steel Reinforcement in Concrete*, Report No. MI-181, Ontario Ministry of Transportation, November 24, 2000.

62. Pianca, F., *Assessment of Stainless Steel Clad Reinforcement for Ministry Use*, Concrete Section, Materials Engineering and Research Office, Ontario Ministry of Transportation, December 2000.